AD- 16830

CODE 25

UNCLASSIFIED

UNIVERSITY OF CALIFORNIA

INSTITUTE OF ENGINEERING RESEARCH

BERKELEY, CALIFORNIA

PROGRESS REPORT
for the year June 27, 1952 to June 27, 1953
Contract No. DA-11-190-Eng-3

SNOW ICE AND PERMAFROST
RESEARCH ESTABLISHMENT
Corps of Engineers
U. S. Army
1215 Washington Ave.
Wilmette, Illinois

SERIES NO 82

ISSUE NO 1

DATE June 2 1953

PROGRESS REPORT
FOR THE YEAR ENDING
JUNE 27, 1953

FACULTY INVESTIGATORS

R. V. Dunkle J. T. Gier

PERSONNEL

A. J. Test	Coordinator
J. T. Bevans	Project Engineer
G. A. Etemad	Engineer
M. Ardalan	Engineering Aid
G. Lee	Engineering Aid
A. Pippen	Engineering Aid
T. Trozera	Engineering Aid
H. Yim	Engineering Aid

INTRODUCTION

Thermal radiation research in the Department of Engineering of the University of California at Berkeley has embraced many phases of radiant energy transfer. (See Gier(1939) and (1940); Boelter (1945); Thermal Radiation Project (1948a,b,c), (1949a,b,c) and (1950))

The Snow Characteristics Research Contract No. DA-11-190-ENG-3, with the Snow, Ice and Permafrost Research Establishment of the Corps of Engineers of the U.S. Army began on June 27, 1952. The basic activities under this contract are as follows:

1. A study of the spectral characteristics of wet and dry snow and the total emissivities and absorptivities of wet and dry snow for temperatures between 0°C and -60°C.

2. A related investigation; the study of the radiant characteristics of various types of paints and materials which might be used in arctic conditions.

3. Determination of criteria for the selection of materials, coatings and clothing for arctic camouflage and for identification under arctic whiteout conditions.

This report summarizes the progress which has been made in these activities to date.

The report is divided into sections (corresponding to the above objectives) discussing the various phases of the activity.

The following indicates the sections included in this report together with a short summary of each section.

I. Spectral Reflectivity and Reflectance of Various Materials

A. Heated Cavity Reflectometer

This section is in relation to item (2) under basic activities above and contains a description of the heated cavity reflectometer as well as spectral reflectance data of materials which can be

coated or painted on a conductive surface or, on the other hand, materials which are conductive and have a fairly high tensile strength. The discussion relates to limitations of the system, analysis of several of the curves, and an example of how the data can be utilized.

B. Paraboloid Reflectometer

The measurement of spectral reflectance data with the heated cavity reflectometer is described in section I-A. As the brief summary indicates, there is a limitation on the materials which can be tested. The paraboloid reflectometer will be built to permit the measurement of spectral reflectance for materials other than those described above. This section of the report includes a brief description of the paraboloid reflectometer which is now being designed.

II. Surface Emissivity at or Near Ambient Temperature

A. The Two-Radiometer Method

This section is in relation to item (1) above and contains a description of the two-radiometer method for measuring surface emissivity of surfaces at or near ambient temperature. The measurement of emissivity at these temperatures is difficult because the energy emitted by the surface is low. The two-radiometer method is described and relevant equations are presented.

B. Emissivity Meter

The two-radiometer method described in II-A above is a laboratory instrument. In order to permit field determination of emissivity, the emissivity meter was designed. This is a portable instrument. This section of the report describes the meter and presents the relevant equations.

III. Transmissivity and Absorptivity of Snow

A. Solarimeter and Albedometer

This section of the report describes two devices which were developed in the laboratory to measure the transmission and albedo of snow to solar radiation. Applicable equations are included and preliminary field data are discussed. Also discussed is the hole effect inherent in all measurements of transmission of snow.

I. SPECTRAL REFLECTIVITY AND REFLECTANCE OF VARIOUS MATERIALS

A. Heated Cavity Reflectometer

Introduction - Spectral reflectivity and reflectance data provides flexible information for the determination of total emissivity or absorptivity. By numerically or mechanically integrating the product of the source or surface spectral energy distribution curve and the spectral reflectivity or reflectance of the surface, it is possible to obtain the total reflectivities for materials when irradiated with different sources and, similarly, it is possible to obtain total emissivities or absorptivities for the material at various temperatures. (See Appendix I for further analysis). This procedure is limited by the spectral region covered by the data. At the present time, facilities are available for measurements in the 1.0 to 13.0 micron region only. A General Electric Recording Spectrophotometer will be available soon for measurements between 0.4 and 1.0 micron. A KBr prism is being obtained and this will permit the extension of the infrared measurements from 13.0 to approximately 25.0 microns. It is more difficult to obtain reliable data in this latter region since the energy available is limited by the maximum temperature attainable in the heated cavity (1500°F).

In addition to the above, the spectral data may reveal the presence of distinct absorption bands for the various materials investigated; this information may be useful in connection with certain detection and camouflage problems, as for instance, part (3) of our present contract.

Description - The system used in these measurements is similar to the one previously used (Thermal Radiation Project 1949a and 1950), however, several changes and modifications have been made that are believed to be refinements. It is believed the revised system will yield more precise data.

The basic components of the experimental equipment are a heated cavity in which is placed a water cooled sample and an optical system to direct the energy into an infrared monochromator. For a given wavelength the energy

reflected from the sample is compared to the energy emitted by the cavity. The ratio of the net deflections of the recording system is a direct measure of the spectral reflectivity or reflectance (see Figure I-A-1).

The cavity is a section of 1/4" wall nickel pipe, 4-1/2" O.D. and approximately 5-1/2" long. The bottom is 1/4" nickel plate with a 0.375" to 1.20" tapered hole in the center. The top is constructed of two sections of the same material, pitched 7° from the horizontal. One side of the ridged top provides for insertion of the sample holder. The entire assembly is joined together by the heliarc process to gain strength and to obtain good thermal conductivity. The choice of nickel was made because of strength, thermal conductivity and oxidation resistance at high temperatures. The cavity is supported in the reflectometer case by three positioning rods for accurate alignment and rigid support, and is heated by three separately controlled nichrome wire wound heaters. The side heater consists of two semi-cylindrical 850-watt, 110-volt "Easi-Duty" muffles connected in series. The top and bottom heaters are molded to conform to the cavity configuration and consist of 22 gage Tophet A resistance wire embedded in Sauereisen No. 6 cement. These two heaters are held firmly against the cavity by the rock wool insulating material which fills the space between the heater-cavity assembly and the water cooled outer case.

The temperature distribution of the cavity is measured with four Chromel-Alumel thermocouples peened to the outside surface of the cavity wall. One thermocouple is placed in the region viewed as the reference; another, measures the temperature in the area opposite the sample. The remaining two are on opposite sides of the cavity midway between the top and bottom. The temperature variation is minimized, by control of the heaters, to a maximum of 10°F. Most reflectance and reflectivity data were taken with a 5°F temperature variation. The cavity was, therefore, approximately isothermal and this fact, combined with the dimensions selected according to prescribed criteria (Buckley 1934) resulted in a close approach to ideal black body radiation.

Three first surface flat mirrors and two first surface spherical mirrors with appropriate shielding make up the optical system which collects the energy from the reflectometer and focuses it upon the entrance slits of the Model 83 Perkin-Elmer Monochromator (see Figure I-A-2). A water cooled shield is placed directly below the cavity to prevent energy emitted by the reflectometer case from entering the measuring system. An iris diaphragm is used as a second shield and is placed at the first focus. Both shields are adjustable in three dimensions to insure complete alignment.

The output of the detector located in the monochromator is amplified with a Model 81 Perkin-Elmer A-C Amplifier. The output of the amplifier is fed into a recording potentiometer.

A check on the alignment of the entire system is made by sighting at the sample holder opening with the holder removed. A zero deflection on the recorder indicates the optical line of sight is passing directly through the center of this opening. Comparisons are also made for different sample surfaces with data obtained from the literature and from previous work (Thermal Radiation Project (1949a) and (1950)).

The sample holder is made up of two concentric cooling jackets. The inner jacket contains a tube which directs a high velocity stream of water directly upon the back of the sample disc. The outer chamber serves to cool the sample holder itself and aids in the elimination of edge heat conduction to the sample (see Figures I-A-3, 4). The temperature of the sample disc has been measured several times and found to be approximately 80°F for a water temperature of 65°F. The errors introduced by this temperature rise are discussed in Appendix I.

The sample disc itself is normally 30 aluminum 0.030" thick and 7/8" in diameter. The samples are punched out, polished with a buffing wheel and the thickness of each is recorded. The paint or other coating is applied and the sample again measured in order to determine the coating thickness. In the case of transmittance samples such as [illegible], a [illegible]

of flat black paint is applied to the sample disc. This black paint absorbs the energy which would be transmitted to the polished aluminum, reflected and retransmitted into the optical system giving erroneous readings. In addition, various thicknesses of transmitting samples are run, until the transmission effect has been eliminated. The reflectivity of plastic materials is measured with a metal disc backing the sample to guard against the possibility that the plastic may soften and be punctured by the water jet.

As mentioned previously, the cavity has a ridged top, the two sections are inclined 7° from the horizontal. The sample itself is viewed at an angle 5° from its normal. Consequently, the reflectometer case must tilt ± 12° between readings. This angular displacement is intended to eliminate a possible first reflection coming from the cooler edge of the opening in the bottom of the cavity. Also, this feature reduces the possibility of energy from the surrounds entering the cavity and reflecting from the sample into the system.

Discussion of Results - As was pointed out in the previous section, the reflectometer has been under development for several years. This latest model is believed to have reduced as much as possible, errors and sources of errors. The use of cooling water in and around the system has been increased and it is believed that the method and manner of shielding has been improved. In addition, the cooling of the sample has been made more effective.

The last point regarding the cooling of the sample has been subjected to much thought. As shown in Figure I-A-4, the cooling water is forced against the back of the sample at a very high velocity. The convection coefficient on this surface has been estimated to be higher than 1000 Btu/hrft^2 °F. Calculations show that such a value is necessary in the case of samples having a high absorptivity (see Appendix I). Heating of the sample is very serious as it affects the longer wavelength measurements appreciably. Calculations in Appendix I show the percent relative error at 15 microns for black surfaces for emissivities of 1.0, 0.9 and 0.8. [illegible]

in the measurements.

Other sources of errors are: (1) the stability of the amplifying-recording system, (2) readable accuracy of the recorder, and (3) operator error. Considering the above factors, the data presented is believed to be accurate to ± 0.02 units in the worst case. Thus, a measured value of r equal to 0.10 may be 0.12 or 0.08.

Data are presented in Figures I-A-5 through I-A-21. Two sets of data are included to demonstrate the effect of sample transmissibility. The reflectance of magnesium oxide for two different thicknesses on two base materials are given in Figures I-A-18 and I-A-19. The first figure illustrates the change of reflectance with thickness for a flat black undercoat. The second figure is comparable data for a polished aluminum base material. The higher reflectance measured for the thicker samples is a result of multiple reflections within the oxide and demonstrates the magnitude of this effect. The second set is for titanium dioxide and the comparison is on the basis of comparable thicknesses with different undercoats, Figures I-A-20 and I-A-21. The region from 3 to 8 microns, Figure I-A-20 is one of transmission, whereas from 11 to 15 microns, the reflectance measured is that of the dioxide.

The data presented for coatings such as paints, furnishes a definite demonstration of the importance of the transmission and reflectance of the base material or undercoat. For irradiation from sources in the temperature range 100 to 1000°F, these effects will have a definite and material influence upon the effective emissivity (emittance). For this reason, the results for several materials presented herein must be termed reflectance and not reflectivity. Those materials which do not indicate transmission effects, provide reflectivity data but this is conditioned by the requirement for a specific minimum sample thickness.

The range of data has been limited by the prism available, to 1.0 to 15.0 microns. As mentioned previously, visible reflectivities will be

measured with the G. E. Recording Spectrophotometer and when the KBr prism is secured, measurements will be extended to 25 microns. A quartz prism is available, but has not yet been used. This prism will permit checking the NaCl prism results between 1.0 and approximately 3.5 microns. In addition, quartz will give better dispersion and hence resolution, in this region.

The data presented are the preliminary results obtained with the equipment. Further work is continuing and the plans are to increase the types of samples measured. A large aircraft manufacturer is furnishing samples of various materials and coatings for measurement. This information may enable better selection of materials for use in the arctic. More accurate radiative heat balances may be calculated for cooling and heating of surfaces in the polar regions using the data obtained.

A sample calculation illustrating the use of the information presented, is given in Appendix II. The calculations are for solar irradiation and a surface temperature of 60°F. This illustration is given to demonstrate the utility of spectral data. The source may be of any form as long as the spectral distribution is known. Numerical or mechanical integration is used to evaluate the source and reflection curves and thus obtain the reflectivity of the material as the ratio of the two areas.

B. Paraboloid Reflectometer

Introduction - The measurement of spectral reflectance with the heated cavity reflectometer has been described in Section I-A. As pointed out in the discussion, the temperature rise of the sample may introduce an appreciable error in the measured reflectance of certain samples. Further, the system is not adaptable to the measurement of the spectral reflectance of other materials, such as snow, ice, and permafrost. The need for an instrument which would permit the measurement of reflectance without heating of the sample provided the impetus for the design of the Paraboloid Reflectometer.

Description - A schematic diagram of the planned system is shown in Figure I-B-1. The source may be selected so as to provide maximum energy at various portions of the spectrum, e.g., globar, mercury lamp, incandescent lamp or hohlraum. The energy from the source will be chopped and directed into a Perkin-Elmer Model 83 monochromator, dispersed by the prism and a monochromatic beam will emerge from the exit slits. An optical system will collimate this beam and direct it between the parabolic mirrors where a flat mirror will reflect the energy onto one of the parabolic mirrors which focuses the energy on the sample. The energy reflected by the sample is collected, collimated and directed to the other parabolic mirror. The second parabolic mirror refocuses the energy on a detector. The output of this detector is amplified and recorded in the same manner as the system described in Section I-A, above.

The sample holder will be constructed so as to permit viewing of the sample and of a reference surface alternately. The reference surface is to have a high reflectance.

Discussion - It is believed that this design has the following advantages:

1. Since the energy is chopped before it strikes the surface of the sample, the emission of the sample will not be detected.
2. The total hemispherical, rather than normal reflectance will be measured.
3. The angle of incidence of the monochromatic beam may be varied by changing the position of the flat mirror.
4. The paraboloids may be placed in a cabinet, the temperature of which may be maintained at any desired temperature.

There are two known limitations in the design as outlined. One, the normal reflected energy will not reach the second parabola since it will be intercepted by the sample. Secondly, the construction of a detector which will have the sensitivity required and yet have a short time response. An

enclosed or evacuated detector is not suitable since the detector must detect energy incident upon it from a hemisphere.

Since the fraction of energy intercepted by the sample is very small, it can either be corrected for theoretically, or by an auxiliary mirror system.

From recent investigation of the literature and preliminary experimental work, it is thought that a suitable detector can be constructed.

In summary, it is believed that the paraboloid reflectometer will present a satisfactory solution to the problem of measurement of spectral reflectivity of samples which cannot be tested in the heated cavity reflectometer. In addition, samples which must be maintained at temperatures under 32°F (i.e., snow, ice and permafrost) can be tested when the paraboloids are enclosed in the controlled temperature cabinet.

A refrigeration unit and required accessories for the controlled environment cabinet have been purchased and the preliminary design of the cabinet completed. The required parabolic mirrors have been received and the front surface aluminized. Accessory optics are available. The optical system will be designed and constructed by September 1, 1953. In the same period of time a detector will be built. It is contemplated that the reflectometer will be placed in operation by October 1, 1953.

II. SURFACE EMISSIVITY AT OR NEAR AMBIENT TEMPERATURE

A. Two-Radiometer Method

Introduction - The measurement of surface emissivities at or near ambient temperature (0 to 100°F) is difficult because the energy emitted by the surface at these temperatures is low. The two-radiometer method (Thermal Radiation Project (1948c)) was developed at the University of California to measure the emissivity of surfaces at these temperatures.

Two radiometers (Gier (1940) and Boelter (1945)) are used to measure the emissivity. One radiometer is heated until it reaches a uniform constant temperature about 30°F above ambient; the other radiometer is unheated and, therefore, its temperature is that of the surrounds. A sample is rotated beneath the radiometers.

By writing an equation for the net interchange between the sample and each of the radiometers, the output of the thermopiles may be related to the emissivity of the surface.

The sample temperature rise is never greater than 5°F.; the actual rise is dependent upon the emissivity of the surface and the speed of rotation of the sample. With such a small temperature rise it is possible to test samples which are subject to deterioration when heated.

Description - A schematic cross section of the experimental apparatus is shown in Figure II-A-1. The detectors are silver-constantan wire wound thermopiles with blackened receiver strips. The case of the radiometer is a section of heavy wall copper tube with an outer case of bakelite. The heated radiometer is wound with a constantan wire heater. The placement of the windings and the large thermal conductivity of the copper reduces the temperature variation along the wall to a maximum of 1/3°F. The internal dimensions of the radiometer case are selected to approach "ideal" Planckian radiation from the opening. The thermopile receiver "sees" this opening with a geometrical shape factor of 0.165. The reference junction of the

thermopile is shielded from the opening by a baffle plate.

Theoretical Analysis - The following assumptions are made:

1. The "hot" radiometer irradiates the sample surface with the intensity σT_H^4.
2. The active receiver strip "sees" the radiometer case opening with a geometrical factor of 0.165. The remainder of the "half-space" viewed by the receiver is occupied by the case.
3. The reference strips sees only the baffle in the radiometer case.
4. The temperature rise of the active receiver strip is small.
5. Convection and conduction losses at the two receiver strips are equal.

A heat balance for each radiometer may be written, neglecting any multiple reflections and assuming the reflectivity is one minus the emissivity.

Heated Radiometer

$$\left(\frac{q}{A}\right)_H = e_H \sigma F(1-e_s)T_H^4 + e_H e_s \sigma F T_s^4 - e_H \sigma F T_H^4 \qquad (1)$$

Cold Radiometer

$$\left(\frac{q}{A}\right)_C = e_C \sigma F(1-e_s)T_C^4 + e_C e_s \sigma F T_s^4 - e_C \sigma F T_C^4 \qquad (2)$$

Where

A = Area - ft^2

e = Emissivity - dimensionless

F = Geometrical form factor - dimensionless

G = Irradiation - $Btu/hrft^2$

K = Radiometer constant - $Btu/hrft^2$ mv

q = Heat flow - Btu/hr

T = Absolute temperature - ^oR

V = Voltage - millivolts (mv)

σ = Stefan-Boltzmann constant - 0.172×10^{-8} Btu/hr ^oR

Subscripts

C = Radiometer at ambient conditions

H = Heated radiometer

s = Sample

The radiometer constant is defined as:

$$\frac{1}{e_H}\left(\frac{Q}{A}\right)_H = K_H V_H = G_H - \sigma F T_H^4 \tag{3}$$

$$\frac{1}{e_C}\left(\frac{Q}{A}\right)_C = K_C V_C = G_C - \sigma F T_C^4 \tag{4}$$

Substitution of (3) into (1) and (4) into (2) gives:

$$K_H V_H = e_s \sigma F(T_s^4 - T_H^4) \tag{5}$$

$$K_C V_C = e_s \sigma F(T_s^4 - T_C^4) \tag{6}$$

Equation (5) may be subtracted from (6) and solved for e_s

$$e_s = \frac{K_C V_C - K_H V_H}{\sigma F(T_H^4 - T_C^4)} \tag{7}$$

Similarly, solving for T_s

$$T_s = \left(\frac{K_C V_C T_H^4 - K_H V_H T_C^4}{K_C V_C - K_H V_H}\right)^{1/4} \tag{8}$$

Equation (7) may be further simplified by the relation

$$T_H^4 - T_C^4 = 4 T_{avg}^3 (T_H - T_C) \tag{9}$$

for $T_H \simeq T_C$.

Equation (7) becomes

$$e_s = \frac{K_C V_C - K_H V_H}{4 \sigma F T_{avg}^3 (T_H - T_C)} \tag{10}$$

The last equation is used in calculation for simplicity and accuracy.

Calibration of Radiometers - The response of the thermopiles are normally assumed to be independent of the source temperature. Although this assumption is satisfactory for the usual applications of radiometers, a more exact

calibration is required when they are used to measure emissivity. Since the calibration constants are a function of temperature, the radiometers are calibrated with "ideal" radiators in the temperature range 0 to 200°F (approximately).

The calibration procedure is as follows:

1. "Ideal" black body radiators are constructed in accordance with established criteria (Buckley (1934)).
2. The radiometer is placed beneath or above the cavity opening, depending on cavity temperature, and readings are made of the thermopile response, radiometer case temperature, and radiator temperature.
3. The net radiation of the thermopile is $F \sigma (T_1^4 - T_R^4)$, where T_1 is temperature of ideal radiator. The constant of the thermopile is computed by expressions analogous to equations 3 and 4, wherein G has been replaced by $F \sigma T_1^4$.

The thermocouples for measurement of the case temperatures are calibrated with constant temperature baths. For temperatures below ambient conditions, baths using mixtures of ice and acetone, ice and water, etc. are used. The radiometers are protected from damage, when immersed in the bath, by thin impervious membranes tightly wrapped about the instrument.

Instrumentation - The thermocouple and thermopile emf's are measured with a Leeds and Northrup Type K-2 potentiometer used with a Type E galvanometer. These instruments are sensitive to 0.3 microvolts, which is 2 percent or less of the smallest reading (thermopile output). The temperatures are referred to an ice junction and precautions taken to reduce stray or thermal emf's that might introduce errors.

Discussion - The equipment described will permit the measurement of the emissivity of snow, ice, frozen ground and other materials used in or natural to the arctic regions. This will be done by placing the radiometers and sample in a deep freeze unit. The data obtained by the two-radiometer method

will augment and substantiate the spectral data described in Section I, above.

Among others, the two-radiometer method will be used to measure the reflectivity of the following surfaces:

1. Snow, artificial and natural;
2. Ice - solid, crushed, etc.;
3. Frozen ground - different types and various moisture contents;
4. Furs - polar bear, white fox, and ermine;
5. Paints; and
6. Metals.

B. Emissivity Meter

Introduction - The two-radiometer method, as described in II-A is a laboratory instrument for the order of magnitude of signals is so small that under field conditions the stray signals would become appreciable and give erroneous determinations of emissivity. This makes it necessary to either test artificial samples or remove actual samples from the region where they are indigenous to the laboratory for testing. Although it is feasible to move most samples, snow in particular presents a problem, since its characteristics vary with time and past history. In view of this fact, a field device has been designed to measure the emissivity of samples. This device is constructed but as yet no tests have been performed. Laboratory calibration and use will soon be underway. It is felt that a thorough check in the laboratory is needed in order that as many sources of error as possible can be eliminated before it is used in the field.

Description - A schematic drawing of the back focussed optical-detector system is shown in Figure II-B-1. The first surface spherical mirror is focussed on the receiver and serves to limit stray energy and to concentrate the energy from the sample. A more detailed drawing of the entire design is shown in Figure II-B-2.

The device consists of a double walled kohlraum for defining the irradiation of the sample surface and the back focused detector. The kohlraum

(or ideal radiator) is a double walled copper cylinder which may be varied in temperature by the use of various coolants. Present plans are to use boiling nitrogen and possibly solid carbon dioxide-isopropyl alcohol mixtures as isothermal fluids. Connections are provided to permit circulation of fluids in the walls of the cavity where such facilities are available, i.e., in the laboratory. The use of low temperatures in the hohlraum eliminates the error introduced by reflection of hohlraum energy from the sample surface. An anticipated difficulty is the possibility that the surface of the sample will freeze by the introduction of the large heat sink. Calculations show this may be partially eliminated by the experimental procedure.

The mirror and focusing tube arrangement permits three dimensional adjustment of the mirror and the thermopile detector. These adjustments are such that they may be easily made in the field if necessary. The optical path is shielded from extraneous energy with an adjustable metal plate. A reference surface may be inserted in the optical path for calibration and operation check. The detector consists of a wire wound silver-constantan 25 junction thermopile supported by nylon-glass fiber threads.

The entire assembly weighs approximately 36 pounds including insulation. This weight is not believed excessive for use in snow. The detector output may be measured with a portable potentiometer such as the L and N Type 8662. As stated before, field tests have not been conducted. It is nevertheless felt the instrument will prove satisfactory for normal field conditions.

Derivation of the Equations - A radiation heat balance written upon the sample surface gives

$$G_T = \epsilon_s \sigma T_s^4 + (1 - \epsilon_s) F_{sh} \sigma T_h^4 + F_{so} (1 - \epsilon_s) \sigma T_\infty^4 \qquad (1)$$

where

G_T = Total energy emitted and reflected from the sample surface

ϵ = Emissivity

T = Absolute temperature - $^\circ R$

F = Shape (or geometrical) factor

σ = Stefan-Boltzmann constant

Subscripts

s = sample

h = hohlraum

o = upper opening in hohlraum

∞ = surrounds (other than hohlraum)

r = receiver

m = mirror

The energy incident upon the receiver is

$$G_r = F_{rm} G_T \qquad (2)$$

where

G_r = Energy incident upon the receiver

F_{rm} = Shape factor of the receiver with respect to the mirror

Values of the shape factors are

$F_{rm} = 0.308$

$F_{s-h} = 1 - F_{s-o} = .974$

$F_{s\infty} = .0262$

Substituting these values in the equation for G_r gives

$$G_r = \sigma (.308) \left\{ \epsilon_s \left[T_s^4 - .974\ T_h^4 - .0262\ T_\infty^4 \right] + .974\ T_h^4 + .0262\ T_\infty^4 \right\} \qquad (3)$$

or

$$G_r = \sigma (.308) \left\{ \epsilon_s (T_s^4) + .974(1-\epsilon_s) T_h^4 + .0262(1-\epsilon_s) T_\infty^4 \right\} \qquad (4)$$

Assuming the following values of temperature

$T_s = 485^\circ R$ $(25^\circ F)$

$T_h = 160^\circ R$ $(-300^\circ F$ - liquid nitrogen)

$T_\infty = 492^\circ R$ $(32^\circ F)$

the value of G_r is

$$G_r = 28.0\ \epsilon_s + 1.15$$

The expected value of ϵ_s ranges between 0.90 and 1.0 and for the lower value, gives

$$G_r = 28.4 \text{ Btu/hrft}^2$$

which will give a detector output of .5 mv with a detector constant of 50 Btu/hrft^2 mv.

Discussion - The advantage of a low temperature hohlraum can readily be seen. Examination of equation (4) for G_r will show that T_h has approximately 40 times the effect of T_∞ as a result of the low value of $F_{s\infty}$; similarly T_h has approximately one-tenth the effect of T_s. Therefore, in order to maintain as high a level of accuracy as possible, T_h must be reduced to a minimum.

III. TRANSMISSIVITY AND ABSORPTIVITY OF SNOW

A. Solarimeter* and Albedometer*

Introduction - The evaluation of heat gains and losses in a snow pack is dependant upon an accurate determination of the heat transfer by convection, conduction and radiation. The problem does not lend itself to simple calculations, since heat flow changes such physical properties of the snow as density, crystal size, shape and hardness, and these changes, in turn, affect the evaluation of heat flow. In view of this, suitable instrumentation is desirable. The albedometer is being developed to measure the heat gains and losses at the surface of the snow pack due to solar radiation, and the solarimeter to measure transmission of solar radiation into the snow pack at any level.

A review of the available data for snow transmission given in SIPRE Report No. 4, reveals a large variation in the attenuation coefficients reported. These efforts of correlation by Lambert's Law of transmission, have necessarily neglected the variables encountered in snow. Consequently, the data are singularly valid for the particular snow cover existing at the time of measurement. There are a large number of physical properties that possibly affect the transmission; the most obvious, density. The extinction coefficient used by chemists (Beer's Law) makes use of the concentration of the absorbing medium. Density is a measure of this concentration. Unfortunately, snow density is variable and frequently a function of depth. Hence the transmission is not an exponential with a linear exponent as in Beer's Law. In addition, snow is a diffuse medium and crystal structure and size is also an important factor to be considered in determining the transmissions. In this connection, a possible variable that would assist in correlation, is the albedo of the snow. The reflectivity of a surface such as snow, is the

*The names chosen to be descriptive of these instruments

sum of the first reflection from the surface alone and the total of the energy passing back through the surface as a result of multiple reflections and transmissions within the snow pack. The albedo is a function of transmission and may serve as one parameter for correlation of transmission with particle size. As a first approximation, one might suggest that the quantitative expression for the attenuation of radiation in passing through this media may be written similar to the expression for atmospheric absorption as follows:

$$\frac{G}{G_o} = e^{-(\alpha + \beta)t}$$

where

G_o = Initial irradiation as indicated by the solarimeter

G = Irradiation at some depth t

α = A scattering coefficient which may be a function of t

β = An absorption coefficient which also may be a function of t

$\alpha + \beta = a$ = An attenuation coefficient

t = Thickness of absorbing medium

An expression similar to the above needs experimental verification. Data may reveal an expression as follows:

$$\frac{G}{G_o} = e^{-a(t)t}$$

An unavoidable, inherent error in the majority of the data reviewed, has been the necessity for forming a cavity in the snow to contain the measuring instruments. In the majority of instances the instruments used for measurements were either photocells or Eppley Pyrheliometers. Both devices required ample space for installation. The cavity causes errors in measurement by virtue of the inter-reflections at the walls of the cavity. In effect, an imperfect black body radiator is formed. The reasons enumerated above led to the adaptation of a silver-constantan wire wound thermopile for measurement of solar transmission. The characteristics desired of the device were:

1. Sensitivity such that it might be used with standard recording equipment without amplification;
2. Flat for easy insertion in the snow without the formation of a cavity;
3. Insensitive to radiation from the surrounds, i.e., long wavelength energy;
4. Rugged and simple for field use; and
5. High transmission and low thermal conductivity.

Description of Basic Features - The essential elements of the device are shown in Figure III-A-1. The thermopile detector (Gier (1939)) is supported in a plastic-glass sandwich. The two junctions of the thermopile are aluminum foil, one blackened and the other white. The plastic case is plexiglas which has a low thermal conductivity. The different pieces are held together with brass screws and sealed with silicone vacuum grease which has proven adequate under field testing. The leads from the thermopile are brought through the plastic to binding posts.

The cover plate used for all instruments to date, is a lantern slide cover glass 3-1/4" x 4". The glass was selected for its transmission characteristics and reproducibility.

The albedometer is merely two receivers similar to those of the solarimeter faced so as to view in opposite directions. The calibration constants are made equal for the two receivers; the output is a measure of the net energy going into the snow pack. If the two are read separately, one measures incident radiation and the other reflected radiation. The albedometer also furnishes a rapid and simple measurement of the albedo of foliage, ground, etc.

Calibration - The instrument was calibrated with a high intensity lamp. The lamp was sighted alternately with a calibrated radiometer which has a glass filter to cut out the long wave radiation of the lamp envelope, and with the solarimeter. The calibration constants obtained were in the order of 12 Btu/hrft^2 mv.

Theoretical Considerations - The basic idea of this device is similar to that of the Eppley Pyrheliometer. The blackened junction has a high emissivity and absorptivity to all wavelengths of energy. The white junction ideally is highly reflectant to solar radiation, but has the same characteristics as the blackened strip for all other radiation. Thus, in the short wavelength (solar) region, the white receiver reflects most of the energy while the blackened strip absorbs a large percentage of the energy. Both absorb equally well in all other regions of the spectrum. Consequently, the instrument is sensitive to solar radiation and insensitive to long wave radiation.

The following table includes the symbols which will be used herein:

V = Thermopile output - mv (eq. 5)

F = Geometrical shape factor - (eq. 12)

G = Irradiation - Btu/hrft^2

K = Thermopile constant - Btu/hrft^2/mv - (eq. 7)

l = Length - ft (eq. 1)

R = Effective reflectivity of a medium or combination of media (eq. 11)

T = Temperature - $^{\circ}$R

v = Thermoelectric power per junction - mv/junction - (eq. 5)

h = Heat transfer coefficient - Btu/hrft^2 $^{\circ}$F (eq. 1)

k = Thermal conductivity - Btu/hrft $^{\circ}$F (eq. 1)

n = Number of junctions (eq. 5)

r = Reflectivity of a surface (eq. 9)

t = Transmissivity of a media (eq. 9)

c = Absorptivity

Δ = Difference

σ = Stefan-Boltzmann constant = .173 x 10^{-8} Btu/hr $^{\circ}$R

Subscripts

L = Long wavelength (low temperature)

S = Short wavelength (solar)

s = Silver

c = Constantan

W = White

B = Black

H = Housing

A = Ambient temperature

Thermopile Calibration Constant - Consider a thermopile exposed to incident energy G.

A heat balance may be written upon the receiver strips as follows:

$$G(\Delta\alpha)_S + \sigma T_H^4(\Delta\alpha)_L = \sigma \alpha_{LB} T_B^4 - \alpha_{LW} T_W^4 + \frac{2k_c}{l_c}(T_B - T_W) + \frac{k_s}{l_s}(T_B - T_H) + \frac{k_s}{l_s}(T_H - T_W) + h(T_B - T_A) + h(T_A - T_W) \qquad (1)$$

The above equation is based on the following assumptions:

1. $T_B > T_H > T_W$ and $T_B > T_A > T_W$
2. l_s = constant
3. l_L = constant
4. $\Delta\alpha_S$ = constant
5. $\Delta\alpha_L$ = constant
6. The shape factor of the device is equal to unity

If it is further assumed that $(\Delta\alpha)_L = 0$ or $\alpha_{LW} = \alpha_{LB} = \alpha_L$, equation (1) becomes

$$G(\Delta\alpha)_S = \sigma \alpha_L (T_B^4 - T_W^4) + \left[\left(\frac{2k_c}{l_c}\right) + \frac{k_s}{l_s} + h\right](T_B - T_W) \qquad (2)$$

A usual simplification is made when $T_B \cong T_W$ as follows (see equation 9, section II-A):

$$T_B^4 - T_W^4 = \frac{(T_B + T_W)^3}{2} (T_B - T_W) \tag{3}$$

Substituting equation (3) into equation (2) yields

$$G(\Delta\alpha)_B = \left[\frac{\sigma \alpha_L}{2} (T_B + T_W)^3 + \frac{2k_o}{l_o} + \frac{k_s}{l_s} + h\right] (T_B - T_W) \tag{4}$$

The output of a thermopile is defined as

$$V = nv(T_B - T_W)$$

Thus

$$\frac{V}{nv} = T_B - T_W \tag{5}$$

Therefore equation (4) now may be written as

$$G(\Delta\alpha)_B = \frac{V}{nv}\left[\frac{\sigma \alpha_L}{2} (T_B + T_W)^3 + \frac{2k_o}{l} + \frac{k_s}{l} + h\right] \tag{6}$$

Which is the form of

$$G = KV \tag{7}$$

where

$$K = \frac{1}{nv(\Delta\alpha)_B}\left[\frac{\sigma \alpha_L}{2} (T_B + T_W)^3 + \frac{2k_o}{l_o} + \frac{k_s}{l_s} + h\right] \tag{8}$$

= calibration constant

Comparison of equations (1), (7) and (8) will show that the assumption of equal long wavelength emissivities for both receiver strips is a critical point in the analysis; from our study of the literature we find that this point has been tacitly assumed or implied in the descriptions of most solar radiation measuring devices.

Also equation (8) reveals that K, the calibration constant will vary with temperature since v, k_s and k_o vary with temperature. Our experiences with thermoelectric devices has indicated that this variation may be appreciable when the device is calibrated at or near normal ambient temperature

(say 70°F) and used at or below freezing temperature. This variation in K should be established before precise evaluations of solar irradiation can be effected. This is another point that has been treated lightly by users of solar radiation measuring devices.

Effect of Plastic Case - The enclosure of the thermopile will affect the detector output. The calibration method used compensates for this effect. An analysis of the magnitude of the influence is made as follows.

Idealize a system of two plane transmitting diffuse media with the thermopile between (see Figure III-A-2).

The value of $G_{1 \text{ to } 2}$ intercepted by the thermopile is from the above figure:

$$G_{1 \text{ to } 2} = G\left(\frac{t_1}{1 - r_1 r_2}\right)$$

The materials used (Plexiglas) have total reflectivities of the order of 5 percent and total transmissivities of 90 percent for solar energy. Therefore

$$G_{1 \text{ to } 2} = G\left(\frac{.9}{1 - .025}\right)$$

$$= .923\ G$$

The effect from a change in transmission of the upper surface can be seen to have a serious result upon the measured values. The transmission has no effect if the value is the same for the calibration source and the source that is being measured. A similar reasoning applies to reflectivities. If the reflectivity of the upper surface is invariant and of the order of 5 percent, changes in the reflectivity of the lower surface have little or no effect upon the value of G_{12}.

Effect of Cavity - As was pointed out previously, a cavity must be formed in the snow to contain the measuring instruments. The cavity causes errors in measurement due to the inner reflections within the cavity. This effect may be approximated by two methods. The first procedure is similar to the preceding analysis (Figure III-A-2).

The value measured by the solarimeter is $G_{1 \text{ to } 2}$

$$G_{1 \text{ to } 2} = G\, t_1 \left[1 + \frac{r_1 R_{23}}{1 - r_1 R_{23}} \right] \tag{10}$$

where

$$R_{23} = r_2 + \frac{t_2 r_3}{1 - r_2 r_3} \tag{11}$$

Assuming:

$t_2 = 0.20$

$r_2 = 0.05$

$r_3 = 0.80$

$r_1 = 0.80$

$\frac{G_{1 \text{ to } 2}}{G} = 1.215\, t_1$

The value which is desired is t_1 actual, whereas the measured value is $1.215\, t_1$. This simplified analysis demonstrates that values much larger than the true transmission may be measured due to the inter-reflections between the instrument and the cavity surfaces.

The second method partially explains the reduced effect from placing the upper surface of the solarimeter in contact with the snow.

A factor F is assumed which by definition is the ratio of energy that is incident upon the cavity lower surface to that which enters the cavity. Therefore, by multiple reflections, the fraction of the total energy incident upon the lower surface is from Figure III-A-3:

$$F + \frac{(1 - F)\, r^2 F^2}{1 - r^2 F(1 - F)} \tag{12}$$

The energy incident upon the lower surface of the cavity approaches F as $F \to 1$. The fraction F can only approach 1 if the cavity is small. Since the solarimeter intercepts only a part of F, the ideal case would be a point. This is impracticable, but the optimum practicable limit would be a cavity t o same size as the solarimeter, i.e., inserting the instrument in

the snow without creating an unnecessary void about it.

Results of Field Tests - Field tests were conducted at the Central Sierra Snow Laboratory during the months of March, April, and a portion of May. Snow conditions were not ideal since this was a melt period and a large amount of free water was present in the snow. The flat upper surface of the instrument did not permit the water to drain properly. The data obtained were primarily useful in determining field performance. The glass to plastic seal was a source of trouble. Leakage of water into the instrument affected the thermopile and developed erroneous readings. A silica-gel drying agent holder was provided in each device, but this was only sufficient to maintain a low water vapor content and not to absorb the water.

The instrument was placed in the snow by two methods. The first was merely direct insertion into the snow, i.e., snow contacts all surfaces. In the other method, a small cavity was made in the snow and the instrument rested on the bottom. The indicated transmission of the same snow cover was approximately 2 times as great by the second method than by the first. This is attributed to the cavity or inter-reflection effect.

The preliminary work indicates that insertion of an unchilled instrument in the snow is not satisfactory. The snow on the upper surface of the instrument melts and refreezes. The freezing effect is eliminated by pre-chilling the instrument to approximately snow temperature before inserting it in the snow.

There were several observations of a sudden increase in recorded output in the positive direction during the early morning hours; these occurred between midnight and 3 AM and lasted for approximately one hour. The output record would suddenly increase, unlike a heating curve, to a value of 0.5 to 1.0 mv and remain constant. At the end of an hour or so, the record would slowly decrease, similar to an exponential cooling curve. Much thought has been given to this action and an attempt will be made to duplicate it with a deep freeze unit so as to determine the possible cause.

Representative results of the aforementioned field tests are tabulated below. These are presented to illustrate the magnitude of the response in millivolts and to demonstrate the practicability of the instrument. As noted previously, the conditions of the test were not ideal and the results given are preliminary in nature. Contemplated plans are to obtain data under more suitable conditions with a more complete knowledge of the variables involved.

DATA OBTAINED AT CENTRAL SIERRA SNOW LABORATORY

Date	Time	Eppley Pyrheli-ometer Btu/hr ft^2	Solar-imeter No. 4 Btu/hr ft^2	Solar-imeter No. 1 Btu/hr ft^2	Percent T Based on Solarimeter *	Remarks
4/1/53	1445	130.3	142.1	11.5	8.1	Light cloud
	1450	121.3	135.0	11.5	8.5	cover
	1505	135.9	168.0	12.0	7.2	
	1520	149.0	186.1	12.0	6.5	
	1535	129.4	182.0	10.6	6.8	
4/2/53	1335	287.0	330.0	19.4	5.9	Bright sunshine
	1430	230.5	267.0	14.4	5.4	
	1545	130.2	214.0	12.7	5.9	
4/4/53	1300	300.0	317.0	30.8	9.7	Bright sunshine
	1315	215.5	320.0	30.8	9.6	
	1620	63.5	63.1	10.5	16.6*	Light clouds
	1640	28.9	31.6	4.9	15.5*	Shade
	1650	21.9	22.8	3.8	16.8*	Cloudy and showers
	1700	14.7	14.8	2.4	16.2*	Cloudy

Constants: 10 junction Eppley Pyrheliometer: 2.50 mv/gm-cal/min/cm^2 or 88.4 Btu/hr ft^2 mv

Solarimeter No. 1: 14.6 Btu/hr ft^2 mv

Solarimeter No. 4: 9.6 Btu/hr ft^2 mv

*All measurements conducted at a level of 4 inches of snow above the instrument, except for the last four measurements, which were at a 2 inch level.

In addition to the above data, points were picked off of the chart roll when the solarimeter was placed at several depths in the same snow bank. A plot of these data reveal a "trend" toward an exponential function although there was considerable scattering. However, it is felt that a refinement of techniques, more complete knowledge of the variables, and improvements in the sensing elements will permit the experimental evaluation of an attenuation

coefficient.

Discussion of Sensing Element - The present design employs flat white paint and flat black paint for the receiver strips. This has not proven satisfactory because these paints do not have identical spectral characteristics in the long wave region, and as has been pointed out, this is the basic assumption upon which the operation of these instruments is predicated. When the long wave emissivity is different, the instrument responds to changes in case temperature as well as short wave radiation. Experimental work is now being conducted to develop coatings with better spectral characteristics.

Another source of difficulty is the glass to plastic seal of the cover plate. To date efforts to obtain a water-tight, temperature resistant seal have been unsuccessful. A change from a glass to a plastic cover has been contemplated and will be made if a seal is not found.

It should be noted that the sensitivity of the solarimeter is approximately two and one-half times that of the 50-junction Eppley Pyrheliometer (12 Btu/hrft^2 mv as contrasted with 28 Btu/hrft^2 mv).

The response of the present instrument as a function of angle has been measured. An example is shown in Figure III-A-4. The response is not the desired cosine function. If a hemispherical cover is used rather than flat glass, the cosine response could be approached to a greater degree, but then the ease of placing the instrument in a snow bank will be lost. The latter feature is the more important due to the errors inherent when a hole must be dug in the snow.

The instrument is subject to fluctuations when gusts of wind cool the case. As described above, the selection of satisfactory receiver strip materials will eliminate the instability. When this defect is corrected, the instrument may be used in the open in the same manner as the Eppley Pyrheliometer.

The transmissivity of the device has been tested and a mean value of 20 percent for the visible region was determined. This value is of the order of

magnitude of previous measurements of transmission of 1 to 2 inches of snow. Consequently, the effect of instrument absorption upon the surrounding snow is small. Similarly, the conduction effect is negligible since the thermal conductivity is approximately 0.1 Btu/hr °F ft.

Future Development - The primary difficulty of the instrument at the present time is its sensitivity to ambient temperature changes. As noted previously, a program is now under way to obtain more suitable receiver materials. In addition to this, a testing program has been outlined to determine other possible difficulties. This program is aimed at:

1. Improving the angular response;
2. Ascertaining the effect of temperature and temperature gradients;
3. Securing a positive seal at all joints;
4. Improving case design; and
5. Determining the weathering effect upon plastic.

This work will be conducted during the summer of 1953 and the improved instrument will be tested during the forthcoming winter. The testing of the device under field conditions is naturally the best and only true test of performance.

Acknowledgement - The field testing was conducted by William H. Parrott of the Central Sierra Snow Laboratory. His suggestions and assistance have been of great value.

REFERENCES

Benford, F. (1946) Radiation in a diffusing medium, Journal of the Optical Society of America, vol 36.

Boelter, L. M. K., R. Bromberg, J. T. Gier, and E. R. Dempster (1945) Use of the thermopile radiometer, N.A.C.A. ARR-XXV.

Buckley, H. (1934) On radiation from inside a circular cylinder, Philisophical Magazine and Journal of Science, vol. 17 (113), series 7, p 876.

Gier, J. T. and L. M. K. Boelter (1939) The silver-constantan plated thermopile, Temperature, Its Measurement and Control in Science and Industry, New York: Reinhold Publishing Company, p. 1284.

Gier, J. T. (1940) Construction and use of a portable radiometer, Bulletin of the American Meteorological Society, vol. 21 (3), p. 113.

Thermal Radiation Project (1948a) Low temperature emissivity measurements, Berkeley: The University of California, Institute of Engineering Research, Report No. 4, Contract No. N7-onr-295, Task I, 37 pages.

Thermal Radiation Project (1948b) Transient behavior of the thermopile radiometer, Berkeley: The University of California, Institute of Engineering Research, Report No. 5, Contract No. N7-onr-295, Task I, 28 pages.

Thermal Radiation Project (1948c) The two radiometer method for the simultaneous determination of emissivity and surface temperature, Berkeley: The University of California, Report No. 6, Contract No. N7-onr-295, Task I, 24 pages.

Thermal Radiation Project (1949a) The absolute spectral reflectivity of certain pigments and metals in the wavelength range between 2 and 15 microns, Berkeley: The University of California, Institute of Engineering Research, Report No. 7, Contract No. N7-onr-295, Task I, 24 pages.

Thermal Radiation Project (1949b) The spectral and total transmissivity characteristics of plexiglas in the wavelength range between 0.4 and 15 microns, Berkeley: The University of California, Institute of Engineering Research, Report No. 8, Contract No. N7-onr-295, Task I, 23 pages.

Thermal Radiation Project (1949c) Non-selective radiometers for hemispherical irradiation and net radiation interchange measurements, Berkeley: The University of California, Institute of Engineering Research, Report No. 9, Contract No. N7-onr-295, Task I, 28 pages.

Thermal Radiation Project (1950) Final report, Berkeley: The University of California, Institute of Engineering Research, Report No. 10, Contract No. N7-onr-295, Task I, 128 pages.

FIGURES

Figure No.	Description
I-A-1	Photograph of heated cavity reflectometer equipment
I-A-2a	Schematic diagram of optical system for the heated cavity reflectometer
I-A-2b	Schematic cross section of heated cavity
I-A-3	Photograph of sample holder
I-A-4	Schematic cross section of sample holder
	(Figures I-A-5 through 21 are spectral reflectivity or reflectance curves from 1.0 to 15.0 microns)
I-A-5	Phosphor bronze, polished Kovar, polished
I-A-6	Molybdenum, polished Zinc, polished
I-A-7	Copper, polished Nickel, polished
I-A-8	Aluminum, polished Aluminum, unpolished
I-A-9	Aluminum, roughened (50 micro-inches) Aluminum foil
I-A-10	Flat black paint (Soysen No. 11) on roughened aluminum Aluminum foil with vinyl chloride coating
I-A-11	Flat black paint (Soysen No. 11) Galvanized iron
I-A-12	Black bakelite Nichrome, Tophet A
I-A-13	Black Glyptal
I-A-14	Red Glyptal
I-A-15	Clear Glyptal
I-A-16	Red Pedigree, protective sealer (P.D. Georgs Co.)
I-A-17	Clear Pedigree, protective sealer (P.D. George Co.)
I-A-18	Magnesium oxide on polished aluminum base
I-A-19	Magnesium oxide on flat black paint base
I-A-20	Titanium dioxide, thin sample

Figure No.	Description
I-A-21	Titanium dioxide, thick sample
I-A-22	Flat white paint, Fuller Decorat
I-B-1	Schematic diagram of paraboloid reflectometer
II-A-1	Schematic diagram of two radiometer equipment
II-B-1	Schematic diagram of optical system of the snow emissivity meter
II-B-2	Schematic drawing of the snow emissivity meter
III-A-1	Exploded view of the solarimeter
III-A-2	Diffusing medium ray diagram
III-A-3	Diagram of cavity inter-reflections
III-A-4	Cosine response of solarimeter

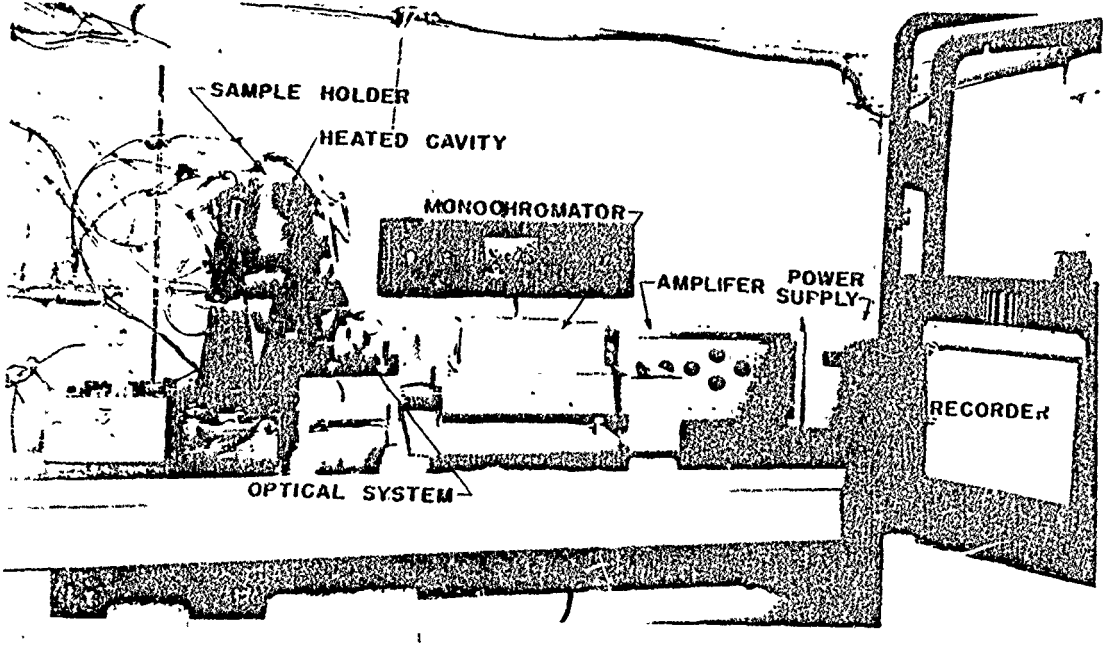
SAMPLE HOLDER
HEATED CAVITY
MONOCHROMATOR
AMPLIFER
POWER SUPPLY
RECORDER
OPTICAL SYSTEM

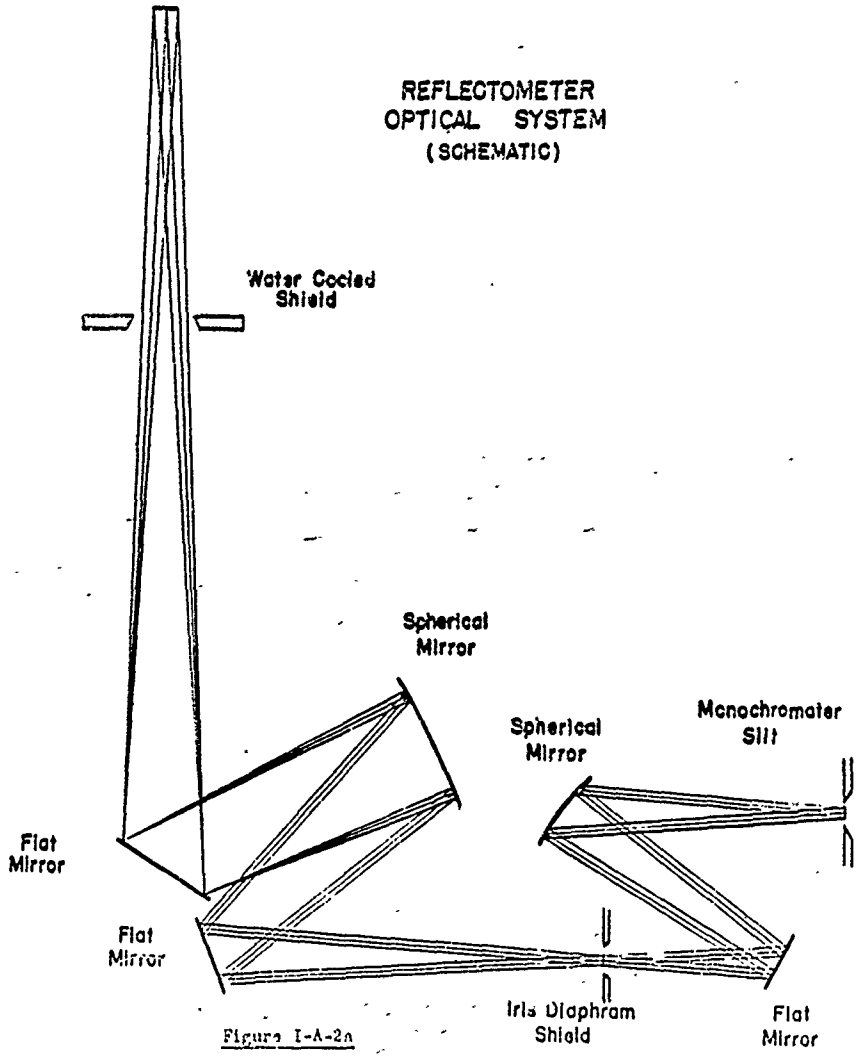
REFLECTOMETER
OPTICAL SYSTEM
(SCHEMATIC)
Water Cooled Shield
Spherical Mirror
Spherical Mirror
Monochromator Slit
Flat Mirror
Flat Mirror
Iris Diaphram Shield
Flat Mirror

Figure I-A-2a

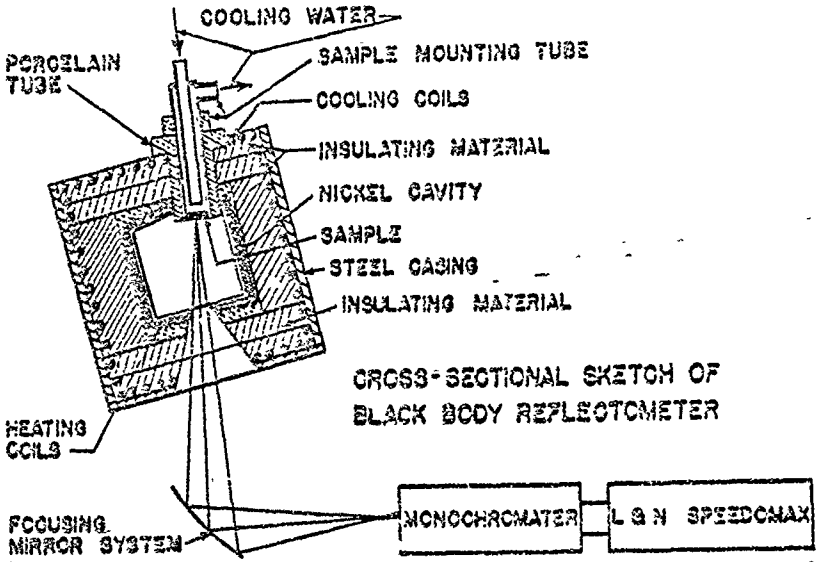

CROSS-SECTIONAL SKETCH OF BLACK BODY REFLECTOMETER

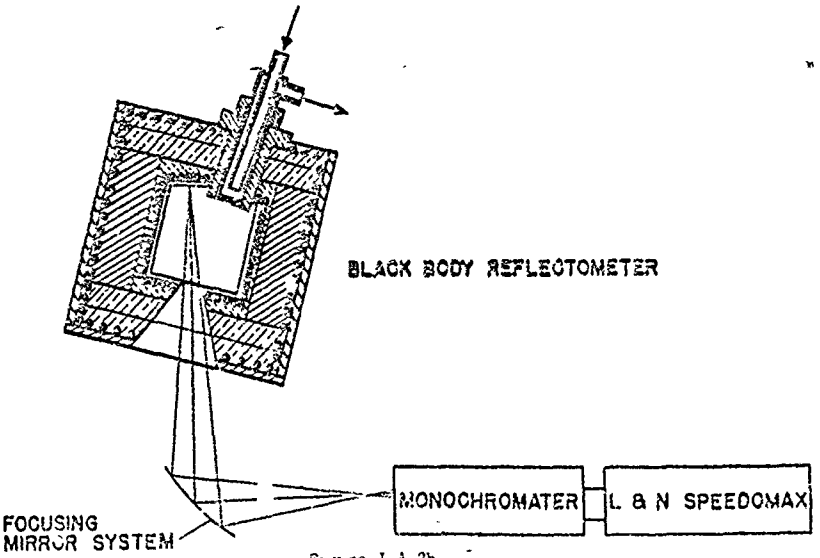

BLACK BODY REFLECTOMETER

Figure I-A-2b

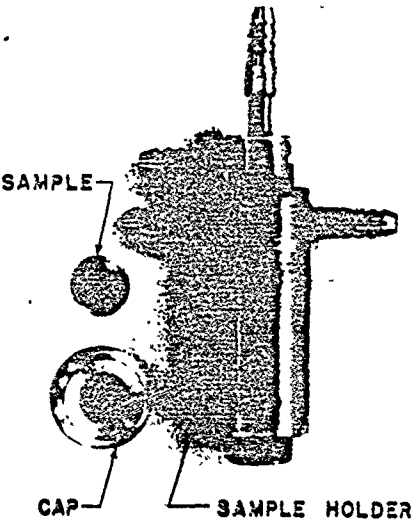
SAMPLE
CAP
SAMPLE HOLDER

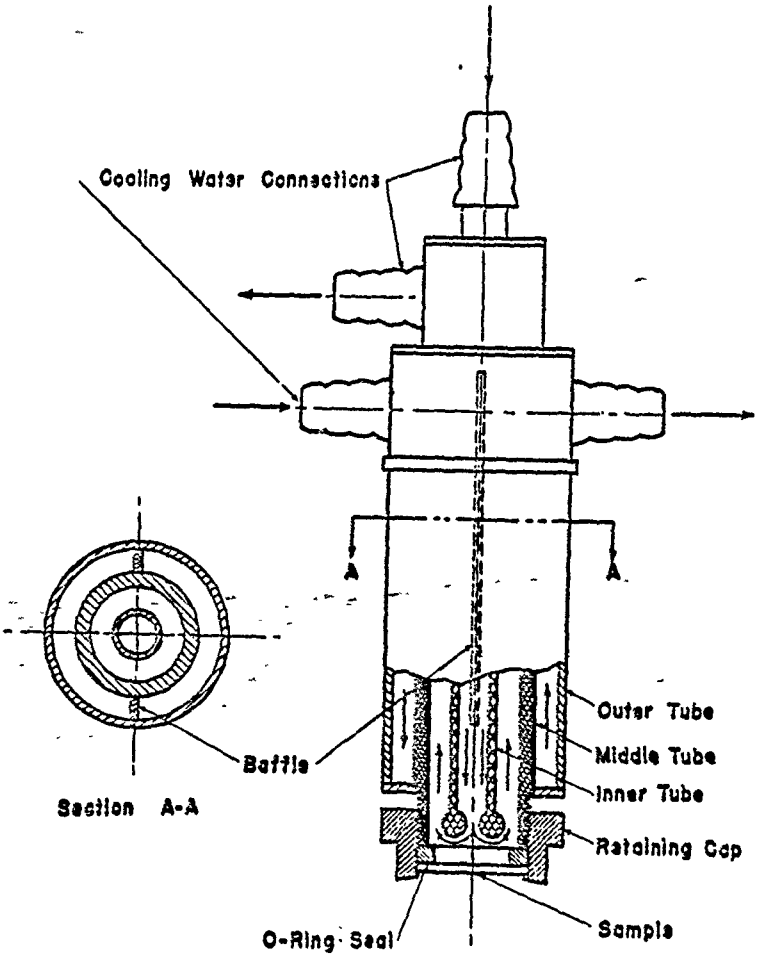

SAMPLE HOLDER

Figure I-A-4

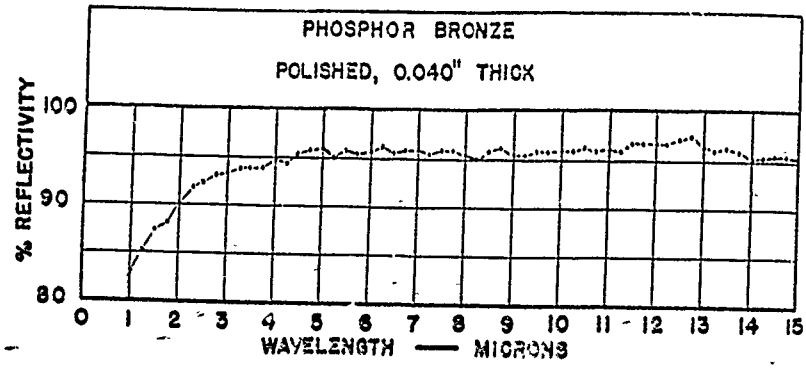
PHOSPHOR BRONZE
POLISHED, 0.040" THICK
% REFLECTIVITY
100
90
80
0 1 2 3 4 5 6 7 8 9 10 11 12 13 14 15
WAVELENGTH — MICRONS

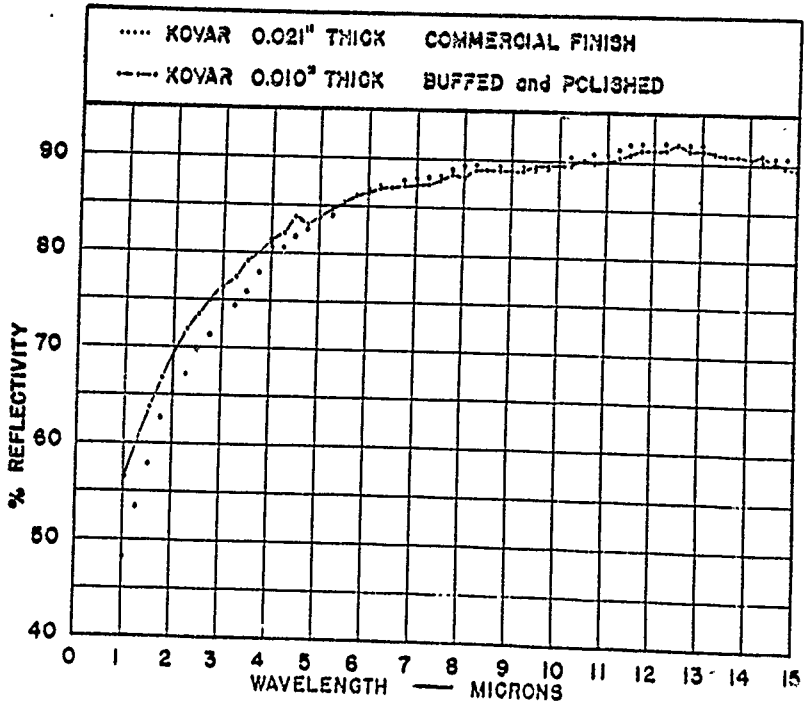
..... KOVAR 0.021" THICK COMMERCIAL FINISH
—·— KOVAR 0.010" THICK BUFFED and POLISHED
% REFLECTIVITY
90
80
70
60
50
40
0 1 2 3 4 5 6 7 8 9 10 11 12 13 14 15
WAVELENGTH — MICRONS

Figure I-A-5

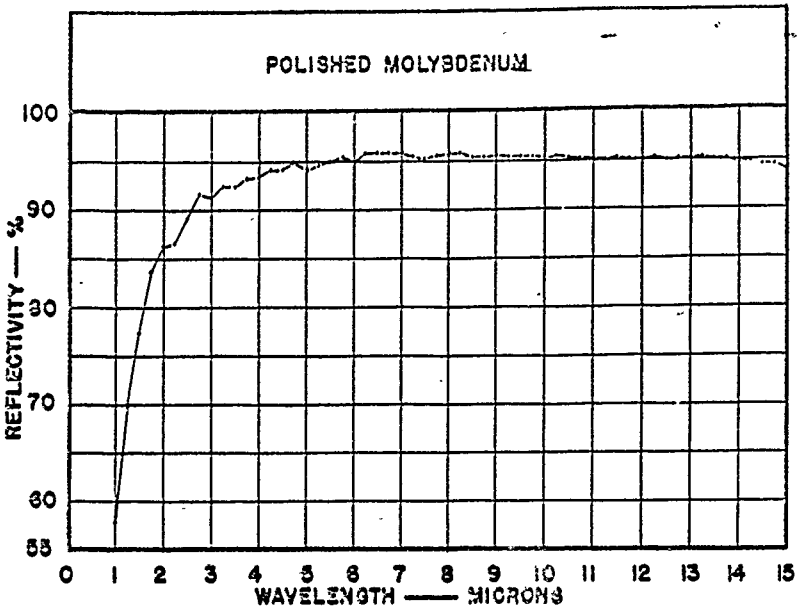
POLISHED MOLYBDENUM
REFLECTIVITY — %
100
90
80
70
60
55
0 1 2 3 4 5 6 7 8 9 10 11 12 13 14 15
WAVELENGTH —— MICRONS

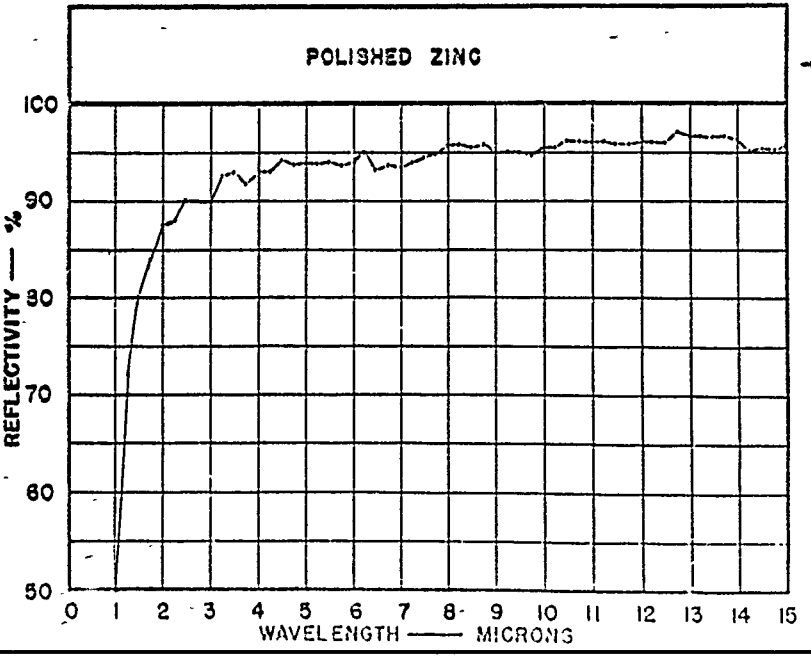
POLISHED ZINC
REFLECTIVITY — %
100
90
80
70
60
50
0 1 2 3 4 5 6 7 8 9 10 11 12 13 14 15
WAVELENGTH —— MICRONS

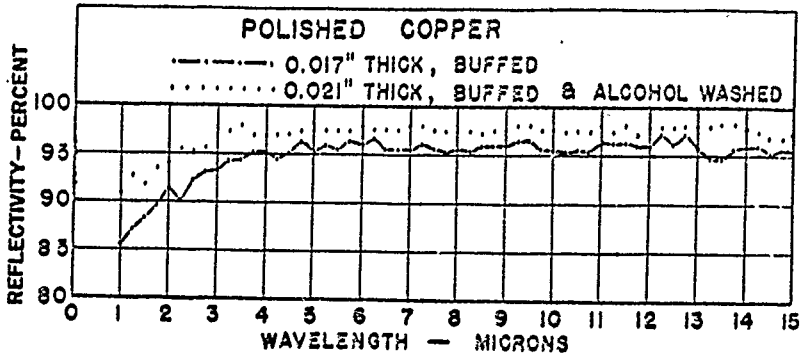
POLISHED COPPER
0.017" THICK, BUFFED
0.021" THICK, BUFFED & ALCOHOL WASHED
REFLECTIVITY-PERCENT
100
95
90
85
80
0 1 2 3 4 5 6 7 8 9 10 11 12 13 14 15
WAVELENGTH — MICRONS

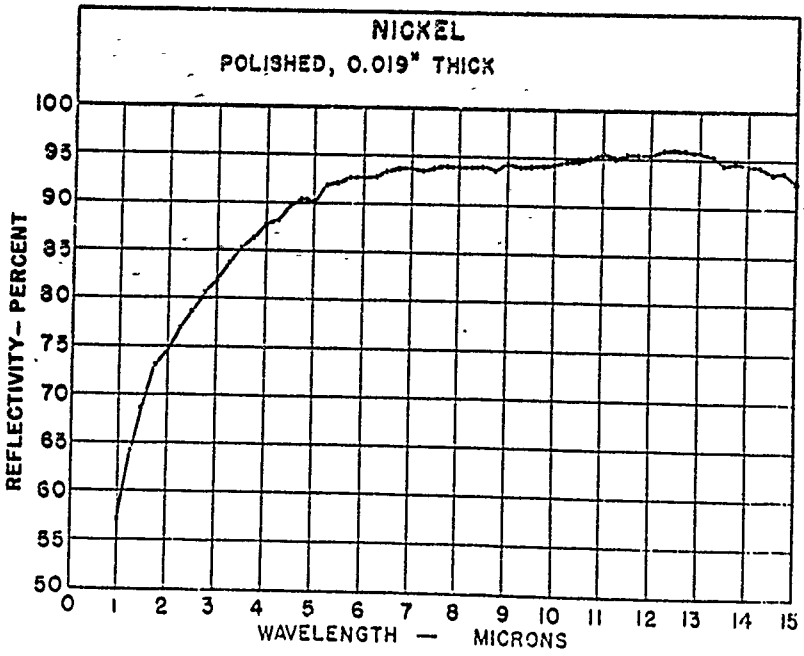
NICKEL
POLISHED, 0.019" THICK
REFLECTIVITY- PERCENT
100
95
90
85
80
75
70
65
60
55
50
0 1 2 3 4 5 6 7 8 9 10 11 12 13 14 15
WAVELENGTH — MICRONS

Figure I-A-2

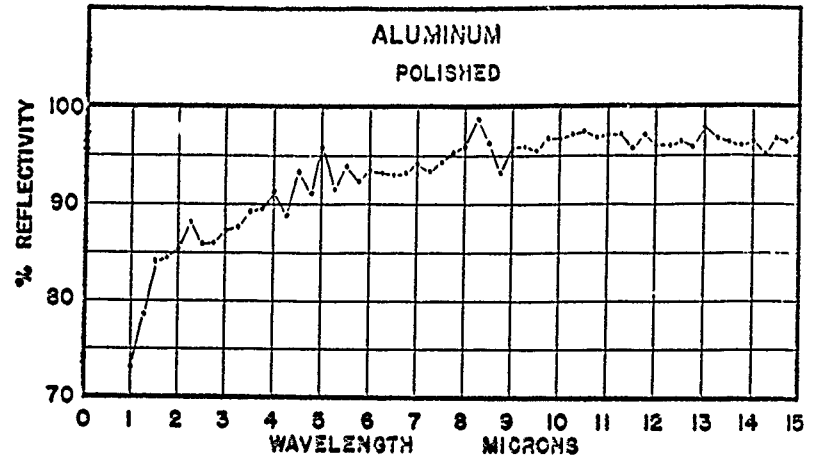
ALUMINUM
POLISHED
% REFLECTIVITY
100
90
80
70
0 1 2 3 4 5 6 7 8 9 10 11 12 13 14 15
WAVELENGTH MICRONS

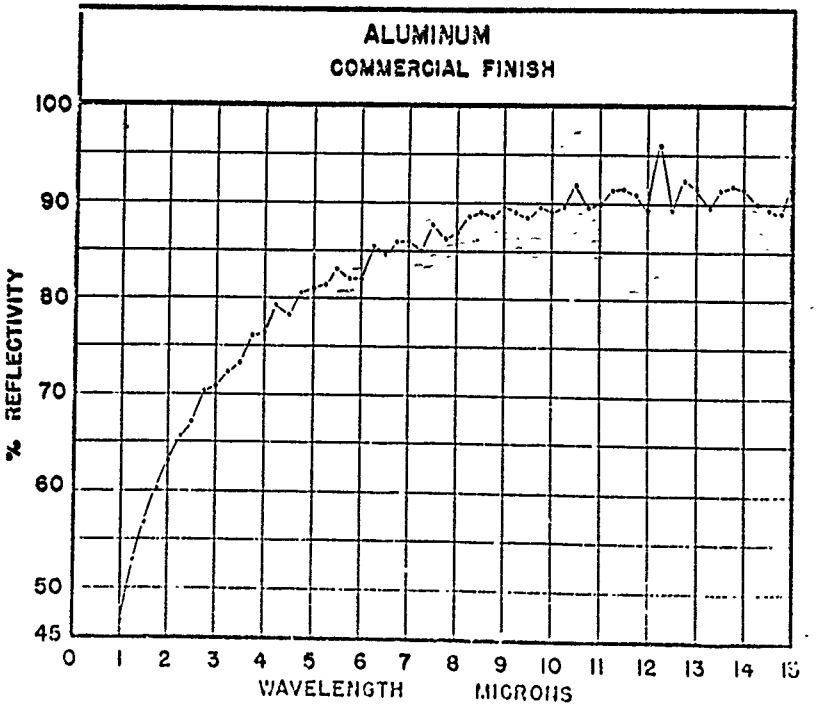
ALUMINUM
COMMERCIAL FINISH
% REFLECTIVITY
100
90
80
70
60
50
45
0 1 2 3 4 5 6 7 8 9 10 11 12 13 14 15
WAVELENGTH MICRONS

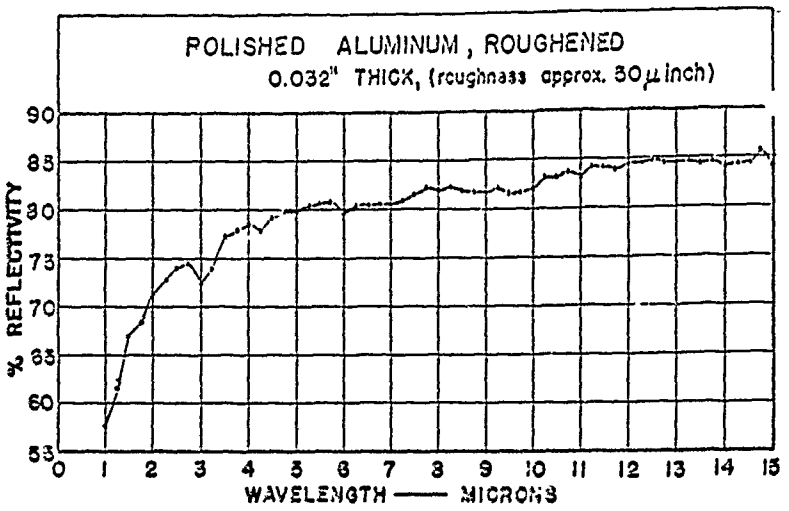
POLISHED ALUMINUM, ROUGHENED
0.032" THICK, (roughness approx. 30μ inch)
% REFLECTIVITY
90
85
80
75
70
65
60
55
0 1 2 3 4 5 6 7 8 9 10 11 12 13 14 15
WAVELENGTH —— MICRONS

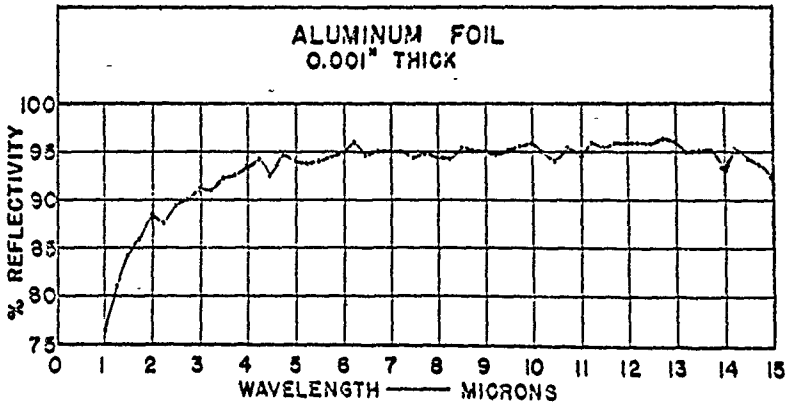
ALUMINUM FOIL
0.001" THICK
% REFLECTIVITY
100
95
90
85
80
75
0 1 2 3 4 5 6 7 8 9 10 11 12 13 14 15
WAVELENGTH —— MICRONS

Figure I-A-9

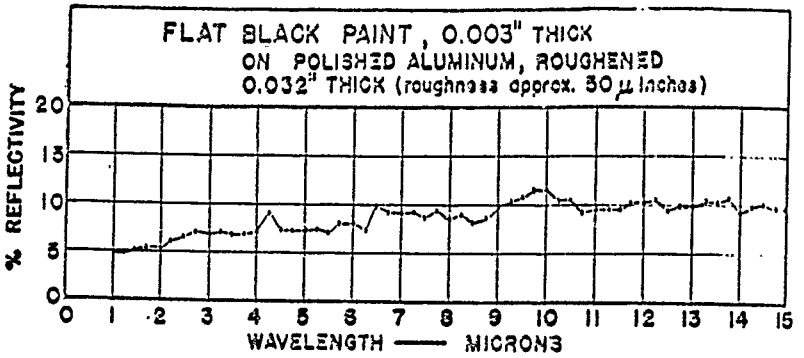
FLAT BLACK PAINT, 0.003" THICK
ON POLISHED ALUMINUM, ROUGHENED
0.032" THICK (roughness approx. 50 μ inches)
% REFLECTIVITY
20
15
10
5
0
0 1 2 3 4 5 6 7 8 9 10 11 12 13 14 15
WAVELENGTH —— MICRONS

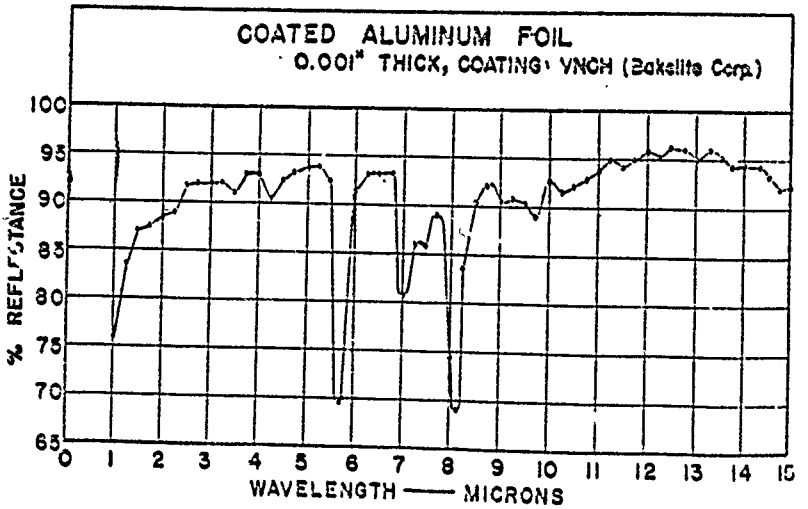
COATED ALUMINUM FOIL
0.001" THICK, COATING VNCH (Bakelite Corp.)
% REFLECTANCE
100
95
90
85
80
75
70
65
0 1 2 3 4 5 6 7 8 9 10 11 12 13 14 15
WAVELENGTH —— MICRONS

Figure I-A-10

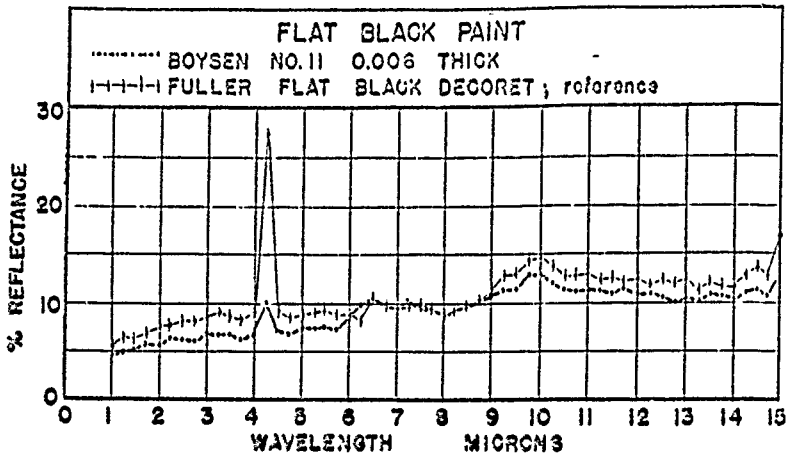
FLAT BLACK PAINT
BOYSEN NO. 11 0.006 THICK
FULLER FLAT BLACK DECORET ; reference
% REFLECTANCE
30
20
10
0
0 1 2 3 4 5 6 7 8 9 10 11 12 13 14 15
WAVELENGTH MICRONS

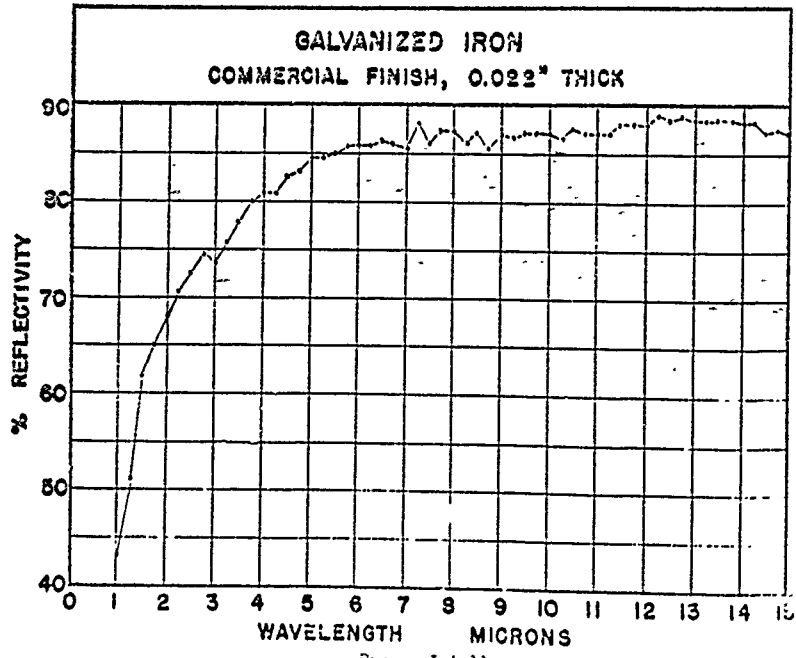
GALVANIZED IRON
COMMERCIAL FINISH, 0.022" THICK
% REFLECTIVITY
90
80
70
60
50
40
0 1 2 3 4 5 6 7 8 9 10 11 12 13 14 15
WAVELENGTH MICRONS

Figure I-A-11

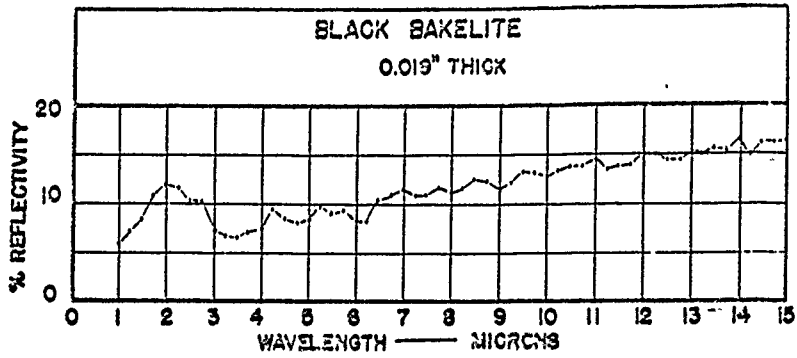
BLACK BAKELITE
0.019" THICK
% REFLECTIVITY
20
10
0
0 1 2 3 4 5 6 7 8 9 10 11 12 13 14 15
WAVELENGTH —— MICRONS

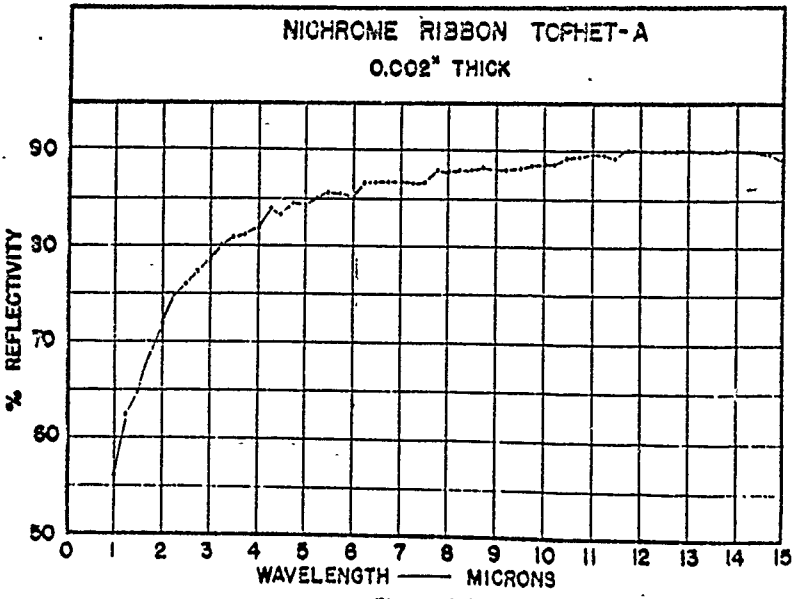
NICHROME RIBBON TOPHET-A
0.002" THICK
% REFLECTIVITY
90
80
70
60
50
0 1 2 3 4 5 6 7 8 9 10 11 12 13 14 15
WAVELENGTH —— MICRONS

Figure I-A-12

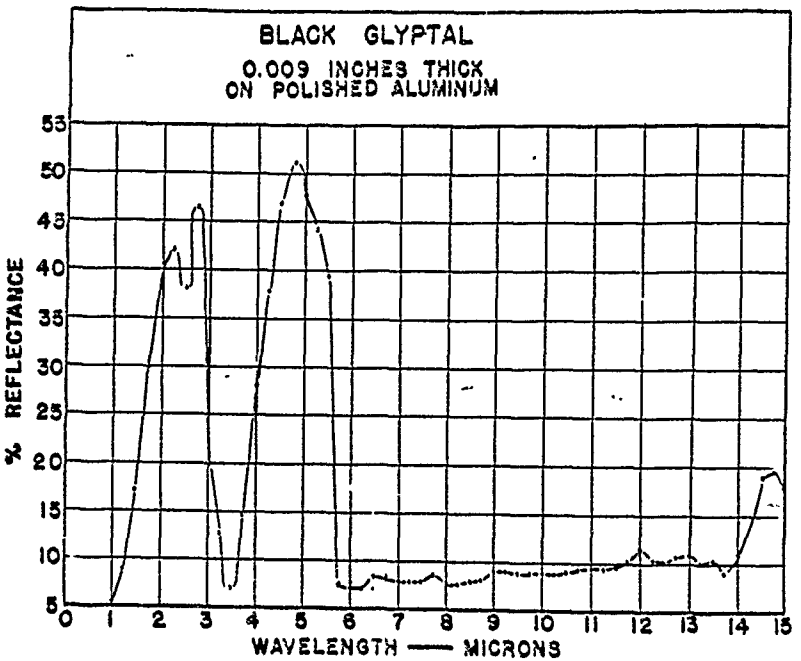
BLACK GLYPTAL
0.009 INCHES THICK
ON POLISHED ALUMINUM
% REFLECTANCE
55
50
45
40
35
30
25
20
15
10
5
0 1 2 3 4 5 6 7 8 9 10 11 12 13 14 15
WAVELENGTH —— MICRONS

Figure I-A-13

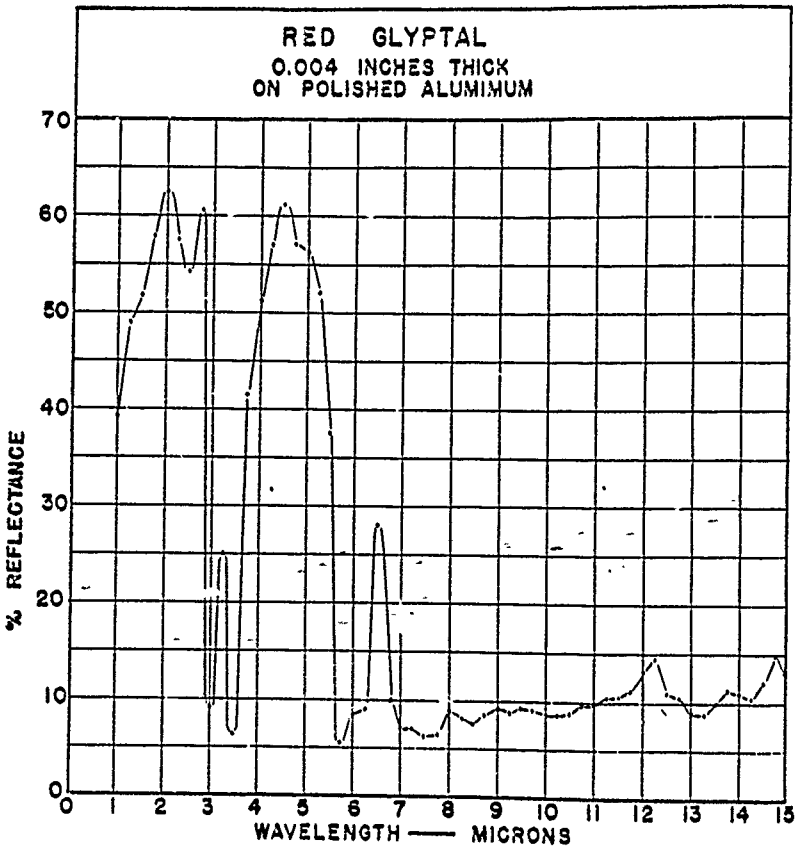
RED GLYPTAL
0.004 INCHES THICK
ON POLISHED ALUMIMUM
% REFLECTANCE
0
10
20
30
40
50
60
70
0 1 2 3 4 5 6 7 8 9 10 11 12 13 14 15
WAVELENGTH —— MICRONS

Figure I-A-14

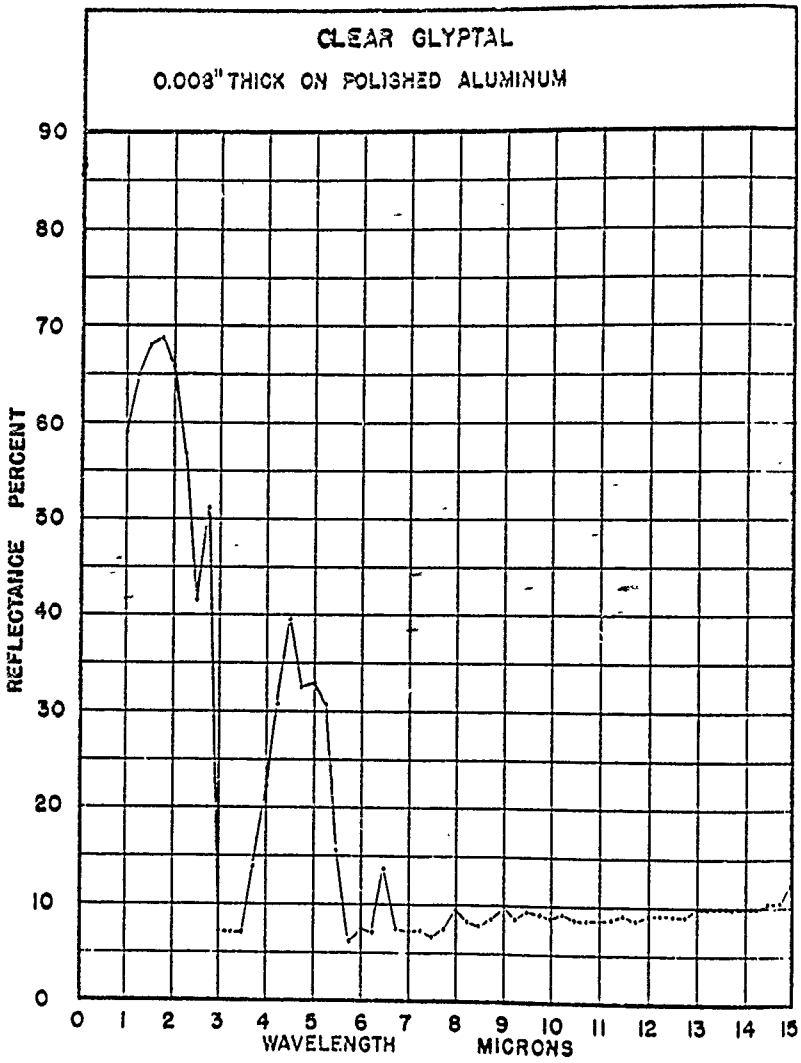
CLEAR GLYPTAL
0.003" THICK ON POLISHED ALUMINUM
REFLECTANCE PERCENT
90
80
70
60
50
40
30
20
10
0
0 1 2 3 4 5 6 7 8 9 10 11 12 13 14 15
WAVELENGTH MICRONS

Figure I-A-15

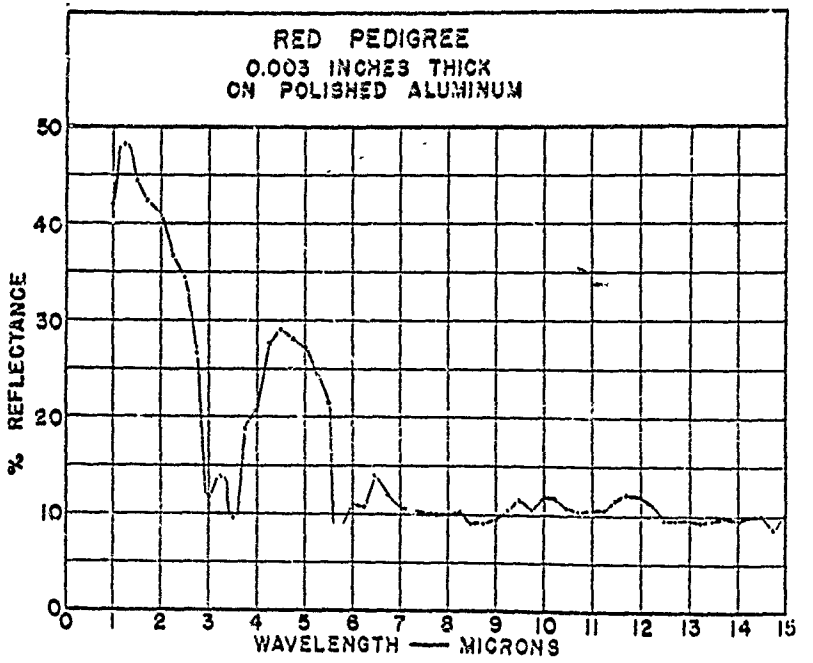
RED PEDIGREE
0.003 INCHES THICK
ON POLISHED ALUMINUM
% REFLECTANCE
50
40
30
20
10
0
0 1 2 3 4 5 6 7 8 9 10 11 12 13 14 15
WAVELENGTH — MICRONS

Figure I-A-16

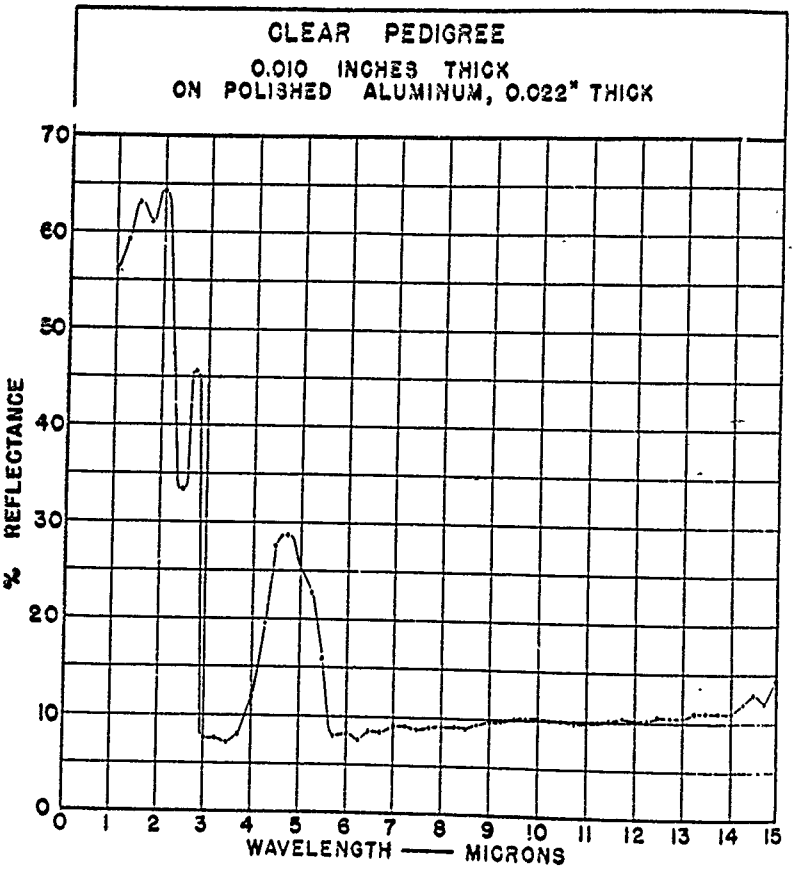
CLEAR PEDIGREE
0.010 INCHES THICK
ON POLISHED ALUMINUM, 0.022" THICK
% REFLECTANCE
70
60
50
40
30
20
10
0
0 1 2 3 4 5 6 7 8 9 10 11 12 13 14 15
WAVELENGTH —— MICRONS

Figure I-A-17

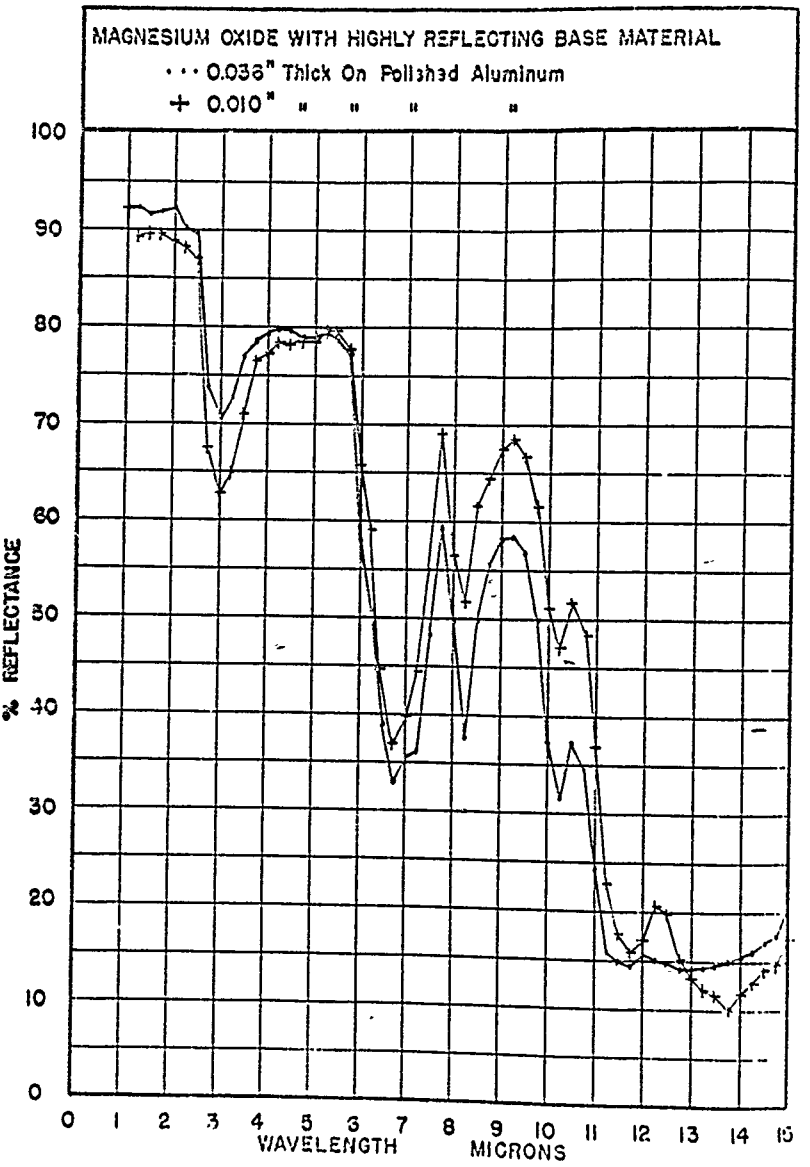
MAGNESIUM OXIDE WITH HIGHLY REFLECTING BASE MATERIAL
• • • 0.036" Thick On Polished Aluminum
+ 0.010" " " " "
% REFLECTANCE
100
90
80
70
60
50
40
30
20
10
0
0 1 2 3 4 5 3 7 8 9 10 11 12 13 14 15
WAVELENGTH MICRONS

Figure I-A-16

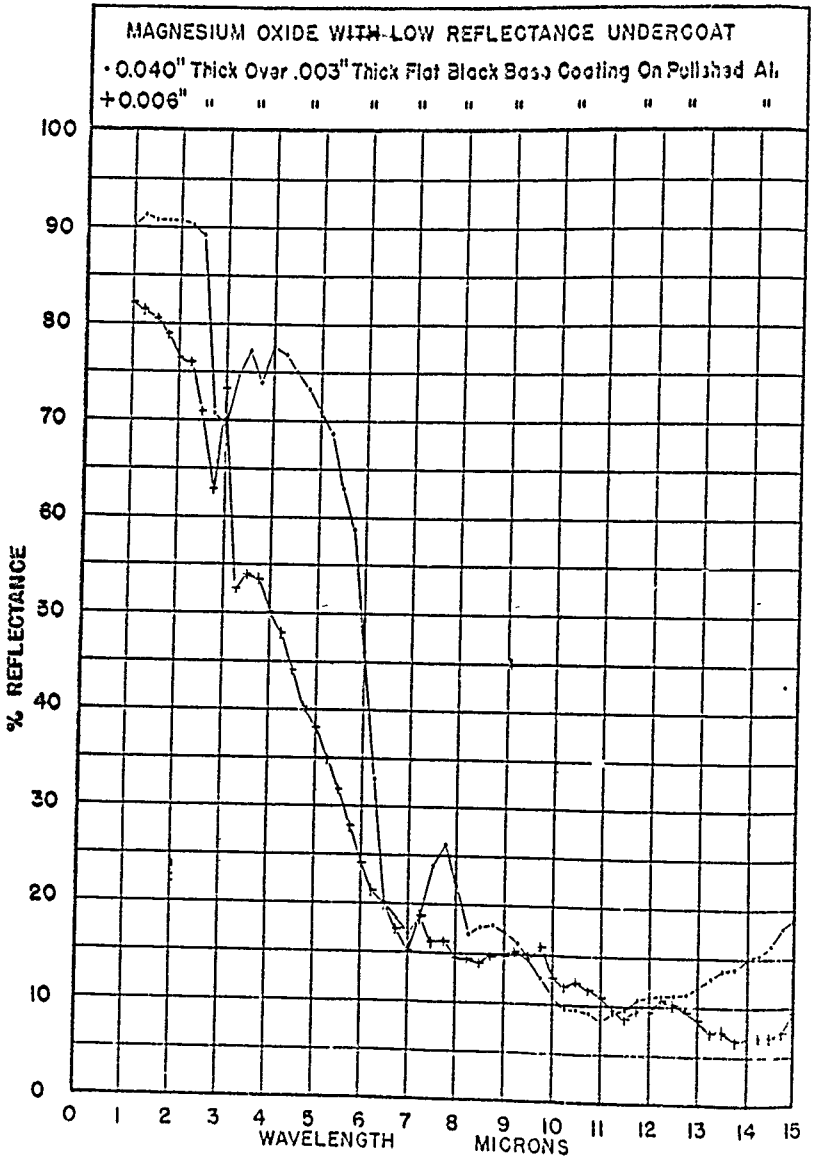
MAGNESIUM OXIDE WITH LOW REFLECTANCE UNDERCOAT
• 0.040" Thick Over .003" Thick Flat Black Base Coating On Polished Al
+0.006" " " " " " " " " " " "
% REFLECTANCE
100
90
80
70
60
50
40
30
20
10
0
0 1 2 3 4 5 6 7 8 9 10 11 12 13 14 15
WAVELENGTH MICRONS

Figure I-A-19

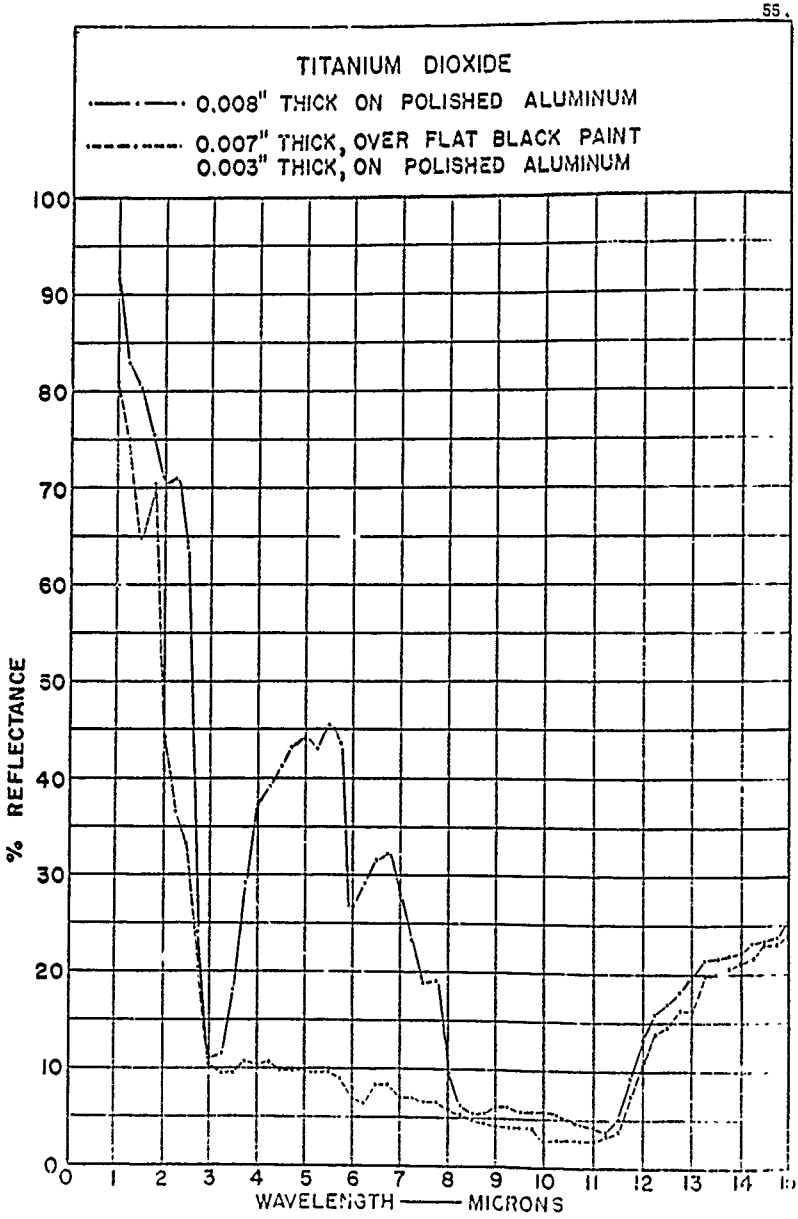
TITANIUM DIOXIDE
0.008" THICK ON POLISHED ALUMINUM
0.007" THICK, OVER FLAT BLACK PAINT
0.003" THICK, ON POLISHED ALUMINUM
% REFLECTANCE
100
90
80
70
60
50
40
30
20
10
0
0 1 2 3 4 5 6 7 8 9 10 11 12 13 14 15
WAVELENGTH —— MICRONS

Figure I-A-20

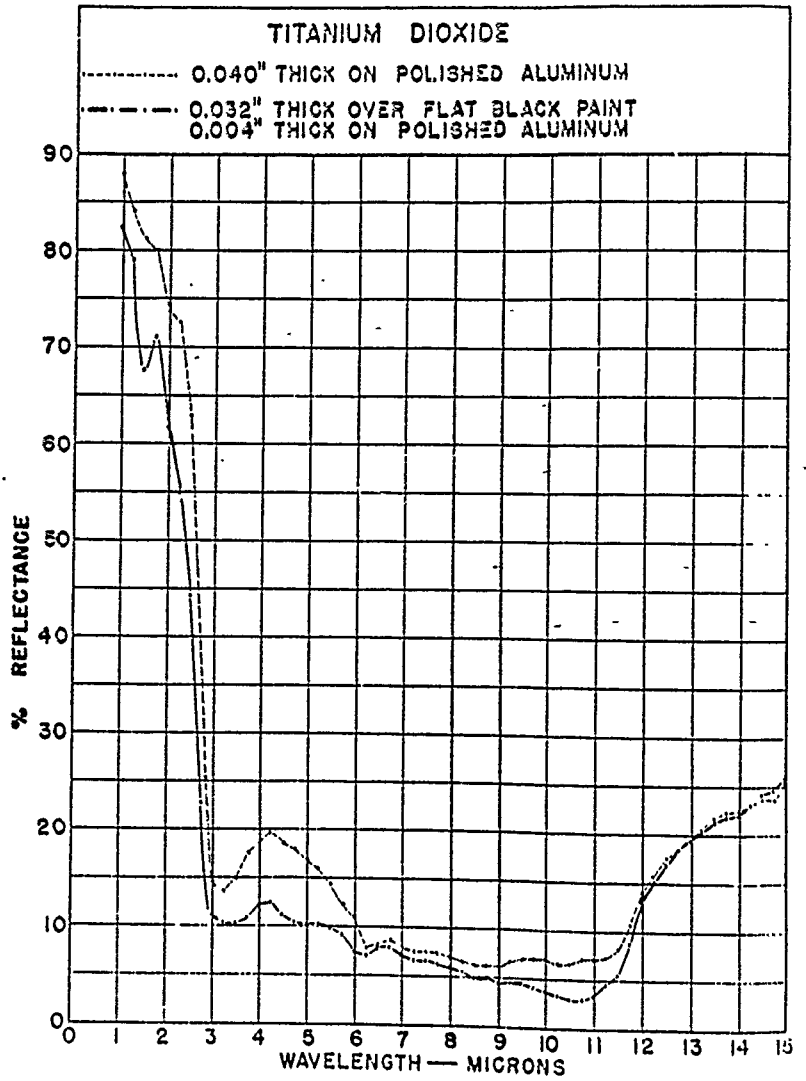
TITANIUM DIOXIDE
0.040" THICK ON POLISHED ALUMINUM
0.032" THICK OVER FLAT BLACK PAINT
0.004" THICK ON POLISHED ALUMINUM
% REFLECTANCE
90
80
70
60
50
40
30
20
10
0
0 1 2 3 4 5 6 7 8 9 10 11 12 13 14 15
WAVELENGTH — MICRONS

Figure I-A-21

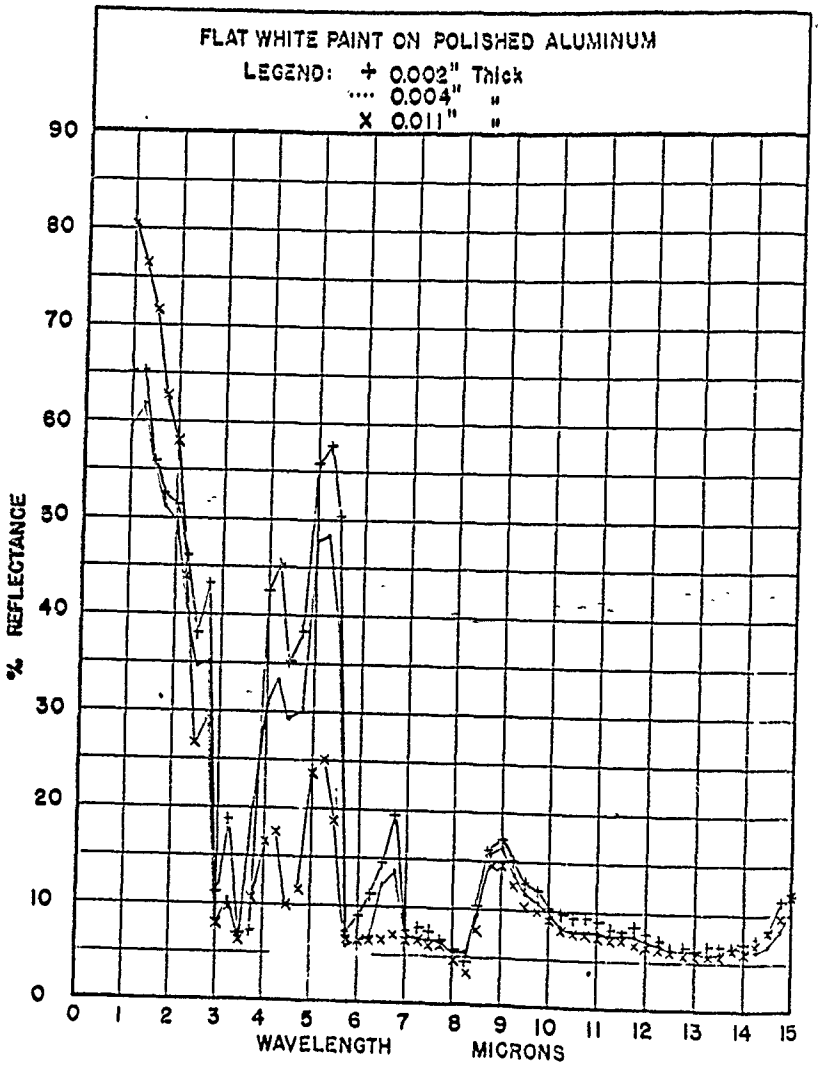
FLAT WHITE PAINT ON POLISHED ALUMINUM
LEGEND: + 0.002" Thick
···· 0.004" "
X 0.011" "
% REFLECTANCE
90
80
70
60
50
40
30
20
10
0
0 1 2 3 4 5 6 7 8 9 10 11 12 13 14 15
WAVELENGTH MICRONS

Figure I-A-22

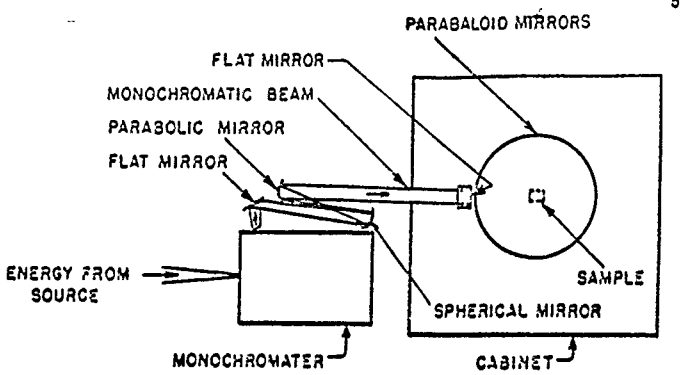

TOP VIEW

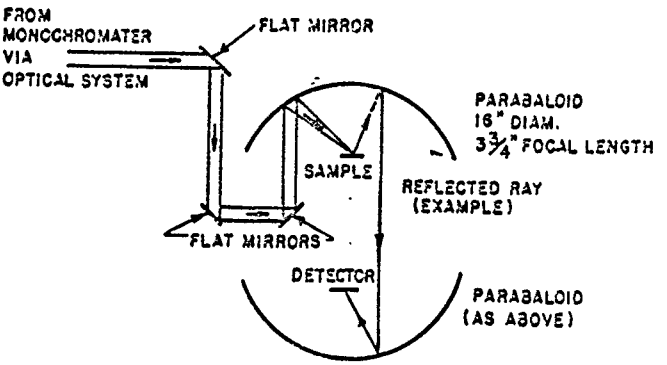

SIDE VIEW OF PARABALOID

SCHEMATIC DIAGRAM OF

PARABOLOID REFLECTOMETER

Figure E-B-1

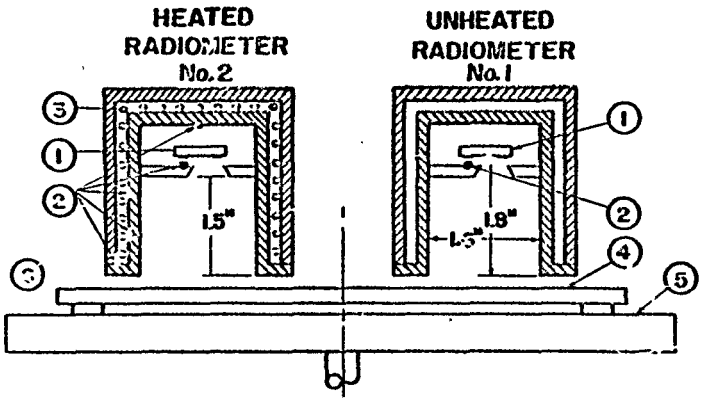

1. THERMOPILE
2. RADIOMETER TEMPERATURE
3. HEATING COILS
4. TEST SURFACE
5. TURNTABLE
6. THERMAL INSULATORS

Figure II-A-1

SNOW EMISSIVITY METER RAY DIAGRAM

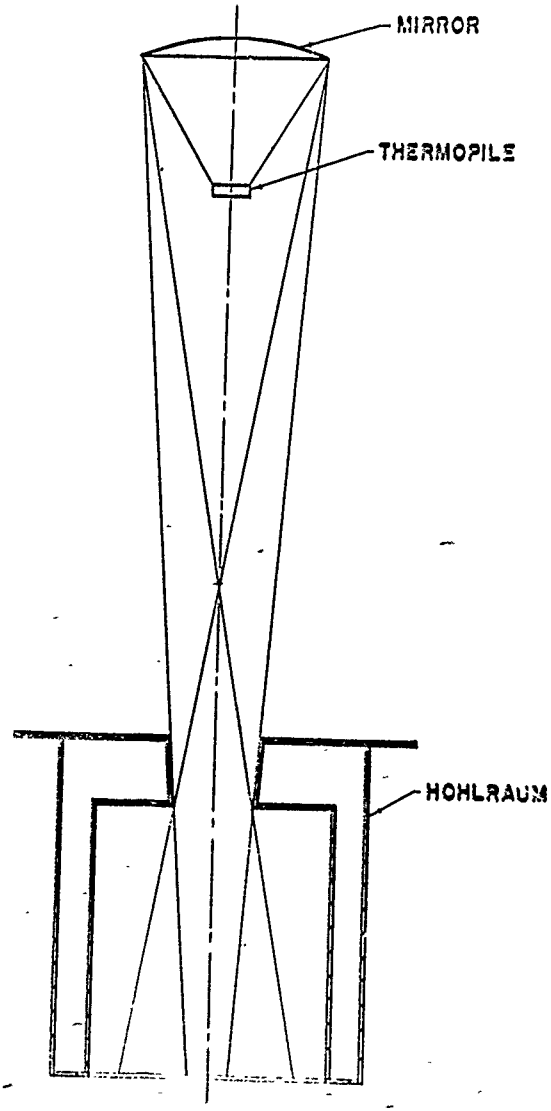

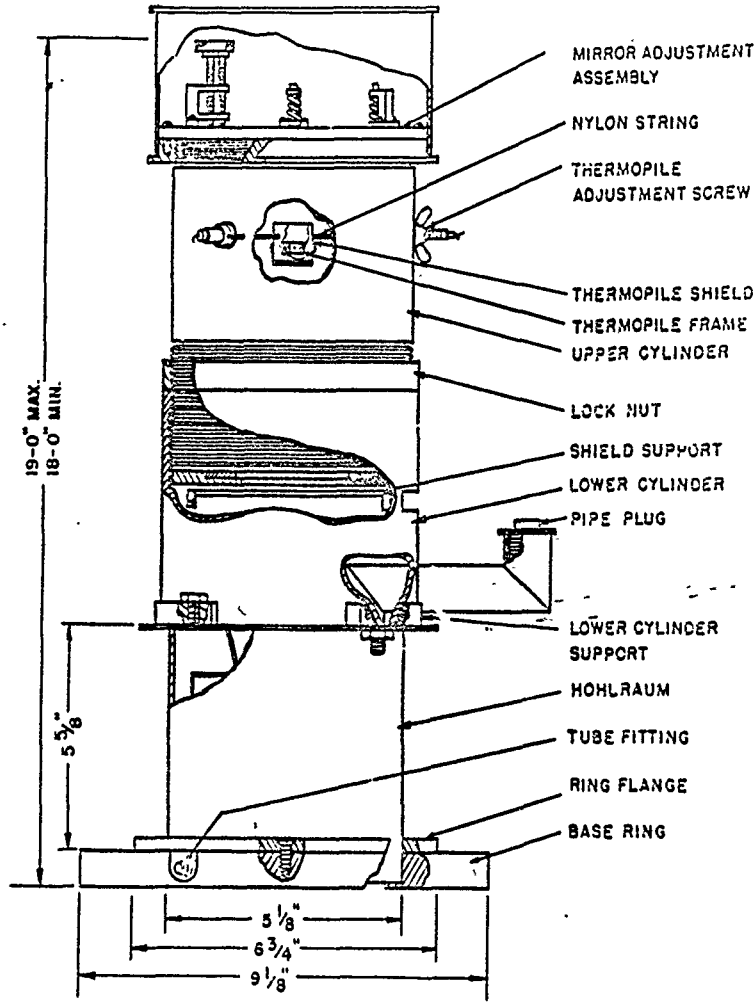

SNOW EMISSIVITY METER

EXPLODED DIAGRAM OF SOLARIMETER

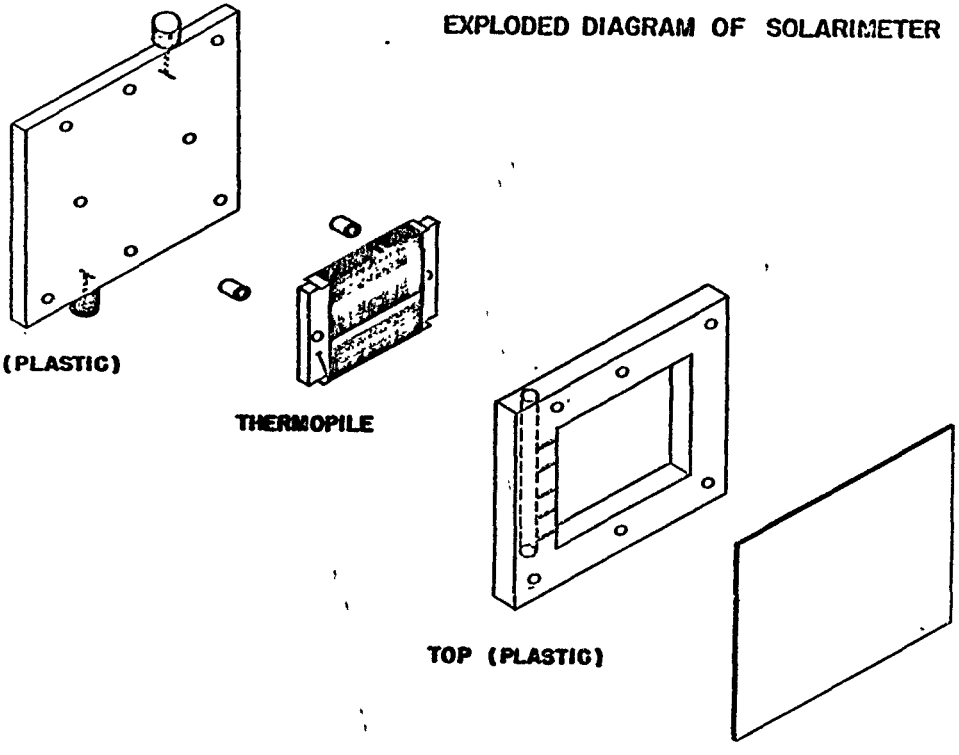

TWO DIFFUSE PLANES

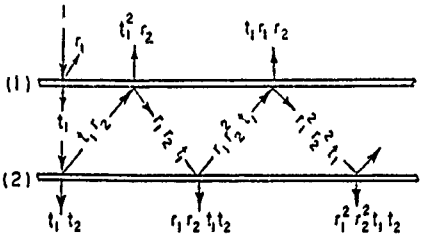

$$T_{1+2} = t_1 t_2 \left[1 + r_1 r_2 + r_2^2 r_1^2 + \cdots\right] = \frac{t_1 t_2}{1 - r_1 r_2}$$

$$R_{1+2} = r_1 + t_1^2 r_2 \left[1 + r_1 r_2 + r_1^2 r_2^2 \cdots\right] = r_1 + \frac{t_1^2 r_2}{1 - r_1 r_2}$$

$$R_{2+1} = r_2 + t_2^2 r_1 \left[1 + r_1 r_2 + r_1^2 r_2^2\right] = r_2 + \frac{t_2^2 r_1}{1 - r_1 r_2}$$

$$\frac{G_{1\ TO\ 2}}{G} = t_1 + t_1 r_1 r_2 + r_1^2 r_2^2 t_1 + \cdots = \frac{t_1}{1 - r_1 r_2}$$

THREE DIFFUSE PLANES

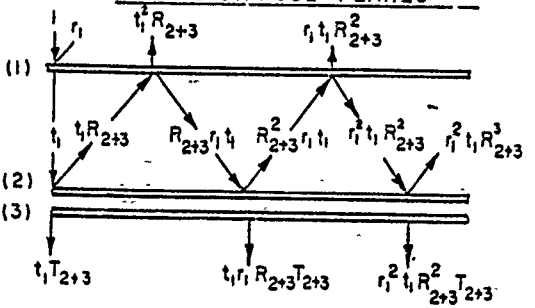

$$T_{1+(2+3)} = t_1 T_{2+3} \left[1 + r_1 R_{2+3} + r_1^2 R_{2+3}^2 + \cdots\right] = \frac{t_1 T_{2+3}}{1 - r_1 R_{2+3}}$$

$$R_{1+(2+3)} = r_1 + t_1^2 R_{2+3} \left[1 + r_1 R_{2+3} + r_1^2 R_{2+3}^2 + \cdots\right] = r_1 + \frac{t_1^2 R_{2+3}}{1 - r_1 R_{2+3}}$$

$$\frac{G_{1+0(2+3)}}{G} = t_1 + r_1 t_1 R_{2+3} \left[1 + r_1 R_{2+3} + \cdots\right] = t_1 + \frac{r_1 t_1 R_{2+3}}{1 - r_1 R_{2+3}}$$

$$R_{2+3} = r_2 + \frac{t_2^2 r_3}{1 - r_2 r_3} \qquad \text{(SEE ABOVE)}$$

$$T = t_2 t_3$$

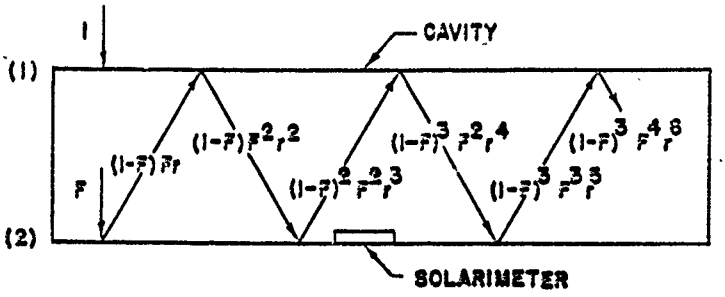

Fraction of energy incident upon lower surface (2) is .....

$$= F + (1-F)F^2r^2 + (1-F)^2F^3r^4 + (1-F)^3F^4r^6 \text{ ----}$$

$$= F + (1-F)F^2r^2\left[1 + (1-F)Fr^2 + (1-F)^2F^2r^4 \text{ ----}\right.$$

$$= F + \frac{(1-F)F^2r^2}{1-(1-F)Fr^2}$$

Figure III-A-3

OBSERVED RESPONSE vs. SOURCE ANGLE

FOR SOLARIMETER

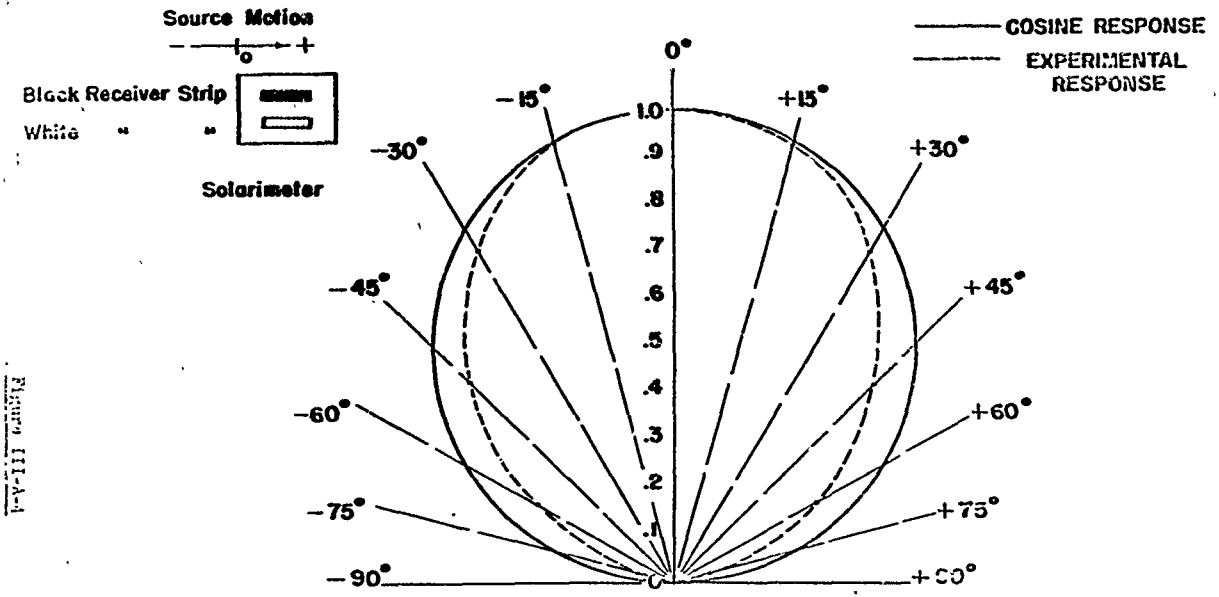

Figure III-A-1

APPENDIX F

Error in Reflectivity Measurements

The reflectivity (or reflectance) measurements are subject to errors introduced by emission from the sample. An estimate of the magnitude of the error may be made as follows:

$$S_a = F(E_{\lambda H} - E_{\lambda 1})$$

$$S_b = F(E_{\lambda H} r_s + e_s E_{\lambda s} - E_{\lambda 1})$$

where

S_a = Recorder deflection when wall of cavity is viewed

S_b = Recorder deflection when sample cavity is viewed

F = Proportionality constant between energy and deflection

E = Emissive power Btu/hr/μ

r = Reflectivity or reflectance

e = Emissivity or emittance

subscripts

H = Hohlraum (ideal radiator)

s = Sample

λ = Wavelength - microns

1 = Datum level for energy interchange

m = Measured

The measured reflectivity is the ratio of S_b to S_a,

$$r_m = \frac{S_b}{S_a} = \frac{E_{\lambda H} r_s + e_s E_{\lambda s} - E_{\lambda 1}}{E_{\lambda H} - E_{\lambda 1}}$$

Assuming that

$$e_s = 1 - r_s$$

then

$$r_m = \frac{r_s(E_{\lambda H} - E_{\lambda s}) + (E_{\lambda s} - E_{\lambda 1})}{E_{\lambda H} - E_{\lambda 1}}$$

$$= r_s \frac{E_{\lambda H} - E_{\lambda s}}{E_{\lambda H} - E_{\lambda 1}} \quad \frac{E_{\lambda s} - E_{\lambda 1}}{E_{\lambda H} - E_{\lambda 1}}$$

$$= r_s \frac{(E_{\lambda H} - E_{\lambda 1}) - (E_{\lambda s} - E_{\lambda 1})}{E_{\lambda H} - E_{\lambda 1}} + \left(\frac{E_{\lambda s} - E_{\lambda 1}}{E_{\lambda H} - E_{\lambda 1}}\right)$$

The error in the measurement, r_s, may be defined as

$$r_m - r_s = \Delta r = (1 - r_s)\left(\frac{E_{\lambda s} - E_{\lambda 1}}{E_{\lambda H} - E_{\lambda 1}}\right)$$

The magnitude of this error at 15 microns will be calculated for sample temperatures of 100°F, 200°F and 300°F, assuming the datum for exchange is 70°F ($E_{\lambda 1}$) and a hohlraum temperature of 1400°F. The maximum error will occur for $1 - r_s = 1$ or $r_s = 0$.

A. Sample Temperature 100°F

$E_{\lambda H}$ = 1670 Btu/hr/μ at 15/μ and 1400°F (Thermal Radiation Project (1950))

$E_{\lambda H}$ = 7.50 Btu/hr/μ at 15/μ and 100°F (Thermal Radiation Project (1950))

$E_{\lambda 1}$ = 6.24 Btu/hr/μ at 15/μ and 70°F. (Thermal Radiation Project (1950))

$$\Delta r_{max} = \frac{E_{\lambda s} - E_{\lambda 1}}{E_{\lambda H} - E_{\lambda 1}} \quad (r_s = 0)$$

$$= \frac{1.26}{1662.5}$$

$$\Delta r_{max} = .000758$$

B. Sample Temperature 200°F

Same as above but,

$E_{\lambda s}$ = 12.3 Btu/hr/μ at 15/μ and 200°F (Thermal Radiation Project (1950))

$$\Delta r_{max} = \frac{6.06}{1662.5}$$

$$= .00364$$

C. Sample Temperature 300°F

$E_{\lambda s}$ = 17.9 Btu/hr/μ at 15/μ and 300°F

$$\Delta r_{max} = \frac{11.66}{1652.5}$$

$$= .007$$

Calculation of Sample Temperature

Consider the sample disk with a paint coating; a uni-dimensional heat balance may be written upon the sample:

$$\frac{q}{A} = \alpha_s \sigma T_H^4 - e_s \sigma T_s^4 = \frac{k_s}{L_s}(T_s - T_2) = h(T_w - T_1)$$

where

$\frac{q}{A}$ = Heat flow through the sample - Btu/hrft^2

T = Temperature - °R

α = Absorptivity

e = Emissivity

L = Thickness - feet

h = Heat Transfer coefficient - Btu/hr °F ft^2

Subscripts

s = Sample

H = Hohlraum

1 = Water side of metal backing disc

2 = Coating side of metal backing disc

w = Water

Evaluating the first term for T_H = 1400°F, T_s = 100°F

$$\sigma\left[\alpha_s T_H^4 - e_s T_s^4\right] = .172\left[\alpha_s(119,600) - e_s(981)\right]$$

Assume

$$\alpha_s = \epsilon_s = 1$$

$$\frac{q}{A} = .172 \left[119{,}600 - 981\right]$$

$$= .172 \left[118{,}619\right]$$

$$= 20{,}400 \text{ Btu/hr}$$

The water side temperature difference is of the order of 20°F (measured). Therefore the water heat transfer coefficient is:

$$h = \left(\frac{q}{A}\right)(T_w - T_1) = \frac{20{,}400}{20}$$

$$= 1020 \text{ Btu/hrft}^2 \text{ °F}$$

The temperature of the surface may be estimated by using assumed values of the thermal conductivity of paints and the corresponding thicknesses.

k_s (Btu/hrft °F)	L_s in.	$T_s - T_2$ (°F)	T_s* (°F)
.1	.005	85	165
	.010	170	250
.2	.005	42.5	122.5
	.010	85	165
.4	.005	21.5	101.5
	.010	42.5	122.5

Sample calculation

$k_s = 0.2$, $L_s = 0.005$ inches

$$\frac{q}{A} = \frac{k_s}{L_s}(T_s - T_2)$$

$$T_s - T_2 = \left(\frac{q}{A}\right)/\left(\frac{k_s}{L_s}\right)$$

$$= (20{,}400)/\left(\frac{.2}{.005}\right)$$

$$= \frac{(20{,}400)(.005)}{(.2)(12)}$$

$$= \frac{20{,}400}{480} = 42.5°F$$

$$T_s = 42.5 + 80 = 122.5°F$$

APPENDIX II

Calculation of emissivities and absorptivities from spectral reflectivity data

A. Emissivity of flat white paint at 60°F.

The spectral reflectivity of flat white paint is shown in Figure I-A-22. For purposes of illustration the data for a thickness of 0.004" will be used.

The reflectivity of a surface is defined as

$$r = \frac{\int_0^\infty r_\lambda E_\lambda \, d\lambda}{\int_0^\infty E_\lambda \, d\lambda} = \frac{\int_0^\infty r_\lambda E_\lambda \, d\lambda}{\sigma T^4}$$

where

r = Reflectivity

E_λ = Emissive power at wavelength λ - Btu/hr micron

λ = Wavelength - microns (μ)

T = Absolute temperature - °R

σ = Stefan-Boltzmann constant = $.172 \times 10^{-8}$ Btu/hr °R^4 ft^2

The above equation may be modified for convenience of calculation to

$$r = \int_0^\infty r_\lambda \frac{E_\lambda}{\sigma T^5} \, d(\lambda T)$$

Values of $\frac{E_\lambda}{\sigma T^5}$ can be readily computed from the Planckian distribution of thermal energy*. Numerical or mechanical integration of the product $r_\lambda \frac{E_\lambda}{\sigma T^5}$ vs λT yields the reflectivity at the temperature T. Thusly,

*Tabulated values of this quantity are to be published soon by R. V. Dunkle

λ	λT	r_λ-%	$\frac{E_\lambda}{\sigma T^5}$	$r_\lambda\left(\frac{E_\lambda}{\sigma T^5}\right)$
2.00	1040	49.6	0	0
2.25	1170	40.5	.001	.0041
2.50	1300	34.6	.005	.00173
2.75	1430	35.1	.0194	.0068
3.00	1560	7.9	.05	.0040
3.25	1690	10.4	.12	.0125
3.50	1820	6.2	.21	.0130
3.75	1950	20.2	.42	.084
4.00	2080	30.7	.72	.221
4.25	2210	33.2	1.04	.345
4.50	2340	29.3	1.58	.462
4.75	2470	30.3	2.15	.650
5.00	2600	47.7	2.75	1.31
5.25	2730	48.2	3.52	1.695
5.50	2860	38.3	4.20	1.610
5.75	2990	5.8	5.07	.294
6.00	3120	6.3	5.73	.361
6.25	3250	8.6	6.57	.433
6.50	3380	12.3	7.38	.906
6.75	3510	13.6	8.12	1.10
7.00	3640	7.0	8.78	.615
7.25	3770	6.6	9.40	.620
7.50	3900	6.6	10.00	.660
7.75	4030	6.5	10.54	.686
8.00	4160	5.3	11.00	.584
8.25	4290	5.4	11.38	.615
8.50	4420	9.1	11.70	1.10

λ	λT	r_λ-%	$\frac{E_\lambda}{\sigma T^5}$	$r_\lambda\left(\frac{E_\lambda}{\sigma T^5}\right)$
8.75	4550	13.6	12.05	1.88
9.00	4680	16.4	12.23	2.00
9.25	4810	13.5	12.38	1.67
9.50	4940	11.7	12.50	1.46
9.75	5070	10.7	12.54	1.34
10.00	5200	9.5	12.59	1.20
10.25	5330	8.2	12.57	1.03
10.50	5460	7.9	12.52	.98
10.75	5590	7.8	12.44	.97
11.00	5720	7.8	12.32	.96
11.25	5850	7.5	12.20	.913
11.50	5980	7.6	12.03	.914
11.75	6110	7.5	11.88	.889
12.00	6240	7.0	11.70	.818
12.25	6370	6.8	11.48	.758
12.50	6500	6.2	11.27	.698
12.75	6630	6.1	11.10	.676
13.00	6760	6.1	10.85	.661
13.25	6890	5.8	10.61	.615
13.50	7020	5.9	10.40	.613
13.75	7150	6.6	10.15	.670
14.00	7280	6.2	9.92	.614
14.25	7410	6.2	9.68	.600
14.50	7540	6.7	9.44	.632
14.75	7670	8.3	9.20	.762
15.00	7800	10.6	8.94	.945

Performing the above integration, gives a value of

$$\int_{2\mu}^{15\mu} r_\lambda \frac{E_\lambda}{\sigma T^5} d(\lambda T) = 0.057$$

The energy remaining from 15μ to ∞ is approximately 47 percent and as an approximation the reflectivity from 15μ to ∞ may be assumed to be 0.10. This yields a value of r = 0.104,

$$\int_{2\mu}^{15\mu} r_\lambda \frac{E_\lambda}{\sigma T^5} d(\lambda T) = 0.057$$

$$.1\int_{15\mu}^{\infty} \frac{E_\lambda}{\sigma T^5} d(\lambda T) = (.1)(.47) = 0.047$$

$$r = 0.104$$

As noted in the body of the report, Section I-A, a KBr prism will be available soon. This will permit measurements to be made to 25μ which will reduce the error of the approximation. The energy remaining in the region 25μ to ∞ will be only 18 percent at 60°F.

The emissivity or absorptivity of the surface is equal to 1 - r, that is $\epsilon = 0.896$.

B. Solar Absorptivity of Flat White Paint

The calculation is performed in a similar manner as that above

$$\alpha = 1-r = 1 - \frac{\int_0^\infty r_\lambda G_\lambda \, d\lambda}{\int_0^\infty G_\lambda \, d\lambda}$$

where

α = Absorptivity

G = Irradiation - Btu/hrft^2

The spectral distribution of solar energy is available from several references. The tables given in "Illumination Engineering" by Moon were used in the following calculation.

λ	r_λ-%	G_λ	$r_\lambda G_\lambda$
0.4	46.0	.0750	.0345
0.5	83.0	.1463	.1215
0.6	88.5	.1382	.1220
0.7	93.0	.1250	.1162
0.8	92.7	.0960	.089
0.9	93.0	.0752	.070
1.00	92.0	.0635	.0584

λ	r_λ-%	G_λ	$r_\lambda G_\lambda$
1.25	61.7	.0416	.0256
1.50	53.3	.0268	.0143
1.75	51.2	.0196	.0100
2.00	49.6	.0124	.0062
2.25	40.5	.0064	.0026

The calculation yields

$$r = 0.796$$

or

$$1 - r = \alpha = 0.204$$

The spectral reflectivity between 0.4 and 1.0 μ was obtained with a G. E. Recording Spectrophotometer. The discrepancy at $\lambda = 1.0\,\mu$ between the data used in the above calculation and that shown in Figure I-A-22 is due to the differences in thickness of the two samples measured. Two different samples were required for the different methods of measurement. The value used was chosen as the more representative in the region of high solar energy since the solar energy distribution curve is decreasing rapidly beyond 1.0 microns.

Acknowledgement - The preparation of this report has been greatly facilitated by (Mrs.) Donna Evans because of her assistance and suggestions in typing, arrangements and assembly.